Neogene Palynostratigraphic Zonation of the Maranon Basin, Western Amazonia, Peru

Authors: Parra, F.J., Navarrete, R.E., di Pasquo, M.M., Roddaz, M., Calderón, Y., et al.

Source: Palynology, 44(4) : 675-695

Published By: AASP: The Palynological Society

URL: https://doi.org/10.1080/01916122.2019.1674395

PALYNOLOGY
2020, VOL. 44, NO. 4, 675–695
https://doi.org/10.1080/01916122.2019.1674395

Neogene palynostratigraphic zonation of the Maranon Basin, Western Amazonia, Peru

F.J. Parra[a,b,c], R.E. Navarrete[c], M.M. di Pasquo[d], M. Roddaz[a], Y. Calderón[e] and P. Baby[a]

[a]Géosciences-Environnement Toulouse, Université de Toulouse III-Paul Sabatier, Toulouse, France; [b]Laboratorio de Bioquimio-Estratigrafía, Facultad de Geociencias, Universidad Nacional de Colombia, Bogotá, Colombia; [c]Departamento de Bioestratigrafía, Paleosedes EU, Bogotá, Colombia; [d]Laboratorio de Palinoestratigrafía y Paleobotánica, Centro de Investigaciones Científicas y Transferencia de Tecnología (CICYTTP-CONICET-ER-UADER), Diamante, Entre Ríos Province, Argentina; [e]Departamento de Exploración, Perupetro, San Borja, Perú

ABSTRACT
The palynology (150 species of pollen grains, 43 species of spores, eight species of dinoflagellate cysts, five genera of algae, two genera of fungal spores, foraminiferal linings, and copepod eggs) of the Neogene succession in the Marañon Basin, north Peru, was thoroughly investigated for the first time from six industrial wells (Arabela-1X, Maynas-1, Tucunare-1X, Tigrillo-30X, Nahuapa-24X, and La Frontera-1). Six palynozones spanning the Early Miocene to the Early Pliocene were defined. The zones in stratigraphically ascending order are as follows: the Mar-A *Corsinipollenites oculusnoctis* Zone (Aquitanian to early Burdigalian: 23.03–17.71 Ma), delimited by the appearance of *Acaciapollenites myriosporites*, *Retitricolporites wijmstrae* and/or *Corsinipollenites oculusnoctis* and/or the disappearance of *Cicatricosisporites dorogensis* at the base; the Mar-B *Malvacipolloides* (*Echitricolporites*) *maristellae* Zone (Burdigalian: 17.71–16.1 Ma), from *Malvacipolloides maristellae* at the base to the disappearance of *Retitricolporites wijmstrae* at the top; the Mar-C *Mauritiidites crassibaculatus* Zone (latest Burdigalian to Late Langhian: 16.1–14.2/13.9 Ma), from the appearance of *Grimsdalea magnaclavata* at the base to the disappearance of *Retitriporites dubiosus* and/or the appearance of *Crassoretitriletes vanraadshooveni* and/or *Psilastephanoporites tesseroporus*; the Mar-D *Crassoretitriletes vanraadshooveni* Zone (Late Serravallian: 14.2–11.62 Ma), from the appearance of *Crassoretitriletes vanraadshooveni* and/or *Psilastephanoporites tesseroporus* to the disappearances of *Mauritiidites crassibaculatus*, *Bombacacidites nacimientoensis*, and *Cyathidites congoensis*; and the Mar-E *Psilastephanoporites tesseroporus* Zone (Early Tortonian to Late Messinian: 11.62–5.48 Ma) from the disappearance of *Corsinipollenites oculusnoctis* and/or *Cyathidites congoensis* to the disappearance of *Psilastephanoporites tesseroporus* and/or *Siltaria santaisabelensis*. These zones were corroborated by means of events ordination demonstrated using graphic correlation. The Mar-F *Ctenolophonidites suigeneris* Zone (latest Messinian to Zanclean) is described only in the Frontera-1 well from the disappearance of *Psilastephanoporites tesseroporus* to the last record of *Ctenolophonidites suigeneris* and/or *Siltaria hammenii*. This study suggests that Pliocene sedimentation is also recorded in the Western Amazonia of Peru, and provides new palynological information compared with the Mio–Pliocene Solimões, Acre, and eastern Amazonas basins.

KEYWORDS
South America; neotropical palynology; palynological zonation; Neogene; Western Amazonia; Marañon Basin; Peru

1. Introduction

The Marañon Basin is one of the most important basins in Peru in terms of hydrocarbon resources, but despite many decades of active exploration (Calderón et al. 2017a, 2017b; Baby et al. 2018), biostratigraphic research has not been conducted. The Marañon Basin contains Paleozoic and Mesozoic source rocks and Mesozoic reservoirs and subthrust traps. Recent studies by Calderón et al. 2017a, 2017b) have improved understanding and modeling of petroleum systems in this basin, especially regarding the formation and deformation of the subthrust traps. However, uncertainties remain concerning the timing and rate of Cenozoic burial, which forms part of the petroleum kitchen system. This is mainly because the Cenozoic deposits of the Marañon Basin are poorly dated (Roddaz et al. 2010).

The stratigraphic ages of Cenozoic units are generally based on different groups of fossils, including algae (Marocco et al. 1995) and invertebrates, such as mollusks and ostracods, from the Chambira, Pebas, and Solimões formations (Whatley et al. 1998; Muñoz-Torres et al. 2006; Ramos 2006; Wesselingh et al. 2006a; Wesselingh and Ramos 2010), and ostracods, foraminifera, and palynomorphs from the adjacent Solimões Basin (Linhares et al. 2011, 2017, 2019; Leandro et al. 2019), as well as vertebrates (Monsch 1998; Salas-Gismondi et al. 2007). The Pebas/Solimões and Nauta formations were palynologically dated from outcrops and wells in the Solimões and Acre basins (Hoorn 1993, 1994a, 1994b, 2006; Hoorn et al. 1996, 2010a, 2010b, 2017; Rebata et al. 2006a, 2006b; Leite et al. 2016; Leandro et al. 2019; Linhares et al. 2019). These units were also recognized from

CONTACT Francisco Javier Parra fjparran@unal.edu.co Géosciences Environnement Toulouse (GET), Université de Toulouse, CNRS UMR 5563/UR 234 IRD/UPS Toulouse/CNES, 14 Avenue Edouard Belin, 31400 Toulouse, France.

Table 1. Location of the six studied wells: Arabela-1X, Maynas-1, Tucunare-1X, Tigrillo-30X, Nahuapa-24X, and La Frontera-1 in the Marañon Basin. N: number of samples analyzed; UTM (18S) coordinates in meters; depth in feet (1 ft = 0.3 meters).

WELL	N	WEST LONGITUD	SOUTH LATITUD	STUDIED INTERVAL IN FEET			STUDIED INTERVAL IN METERS		
ARABELA-1X	13	492310.37	9770151.59	610	to	3340	185.92	to	1017.98
MAYNAS-1	7	397165.18	9672338.65	2700	to	8030	822.92	to	2447.42
TUCUNARE-1X	11	352533.89	9670010.16	5000	to	7650	1523.93	to	2331.61
TIGRILLO-30X	16	393094.04	9557053.76	5310	to	10680	1648.48	to	3255.11
NAHUAPA-24X	20	575898	9536854	2210	to	6230	673.58	to	1898.81
LA FRONTERA-1	10	536014.05	9303755.13	1180	to	4420	359.65	to	1347.15

the Santa Lucia borehole drilled in the southern Marañon Basin (Hermoza 2004) and from three exploration wells (Jibaro 7/1AB-21-181, Huayuri Sur 15/1-AB-15-184D and Capahuari Norte 9/1AB-3-204) drilled in the westernmost part of the Marañon Basin (Hermoza 2004; Hermoza et al. 2005; Wesselingh et al. 2006a). These well sections were dated via mollusks by Wesselingh et al. (2006a) who also correlated them with palynozones (Hoorn 1993, 1994a).

The Neogene palynozones in South America have mainly been established in Colombian, Venezuelan, and Brazilian basins (Van der Hammen 1956; Germeraad et al. 1968; Regali et al. 1974a, 1974b; Lorente 1986; Hoorn 1993; Jaramillo et al. 2011). More specific palynostratigraphic works have been developed in the Solimões and Acre basins (Hoorn 1994a, 1994b; da Silva et al. 2010; Silveira and Souza 2015, 2016; Leite et al. 2016; Leandro et al. 2019; Linhares et al. 2019). Those paleontological studies have helped to establish correlations between Amazonian basins and to reconstruct Neogene biomass evolution (Wesselingh et al. 2006a; Hoorn and Wesselingh 2010; Jaramillo et al. 2010; Boonstra et al. 2015; Antoine et al. 2016; Jaramillo et al. 2017). However, to date, no detailed palynostratigraphic research has been carried out in the Marañon Basin, and the nature, evolution, and age range of the Neogene palynofloras of this basin remain poorly understood.

This study aims to establish a spore/pollen zonation for the Neogene sediments of the retroarc foreland (most subsiding area; Roddaz et al. 2010) of the Marañon Basin based on the identification of qualitative changes in palynomorphs (spores, pollen, and dinoflagellate cysts) through the intervals sampled in six exploration wells (Table 1 and Figure 1).

2. Geological setting

The Marañon Basin covers approximately 320,000 km^2 (Mathalone and Montoya 1995) and is located between 0°N and 7°30′S and 70 and 78°W in northeastern Peru (Figure 1). It is currently considered a foredeep depozone of the northern Amazonian retroarc foreland basin (Roddaz et al. 2005, 2010). The Huallaga and Santiago basins to the southwest and west, respectively, separate the Marañon Basin from the Subandean zone, and to the northeast the basin is bordered by the Iquitos forebulge (Roddaz et al. 2005, 2010). It continues as the Oriente Basin in Ecuador to the northwest and the Putumayo Basin in Colombia to the north. The Guyanese shield and Solimões Basin border the Marañon Basin to the east. To the south, the basin is bordered by the Ucayali and Acre basins, and to the southeast the Contaya arch separates it from the Ucayali Basin (Roddaz et al. 2005).

The Amazonian retroarc foreland basin system started to form between the late Maastrichtian and early Paleocene, during the first period of Amazonian Andes mountain building (Hurtado et al. 2018; Louterbach et al. 2018). This late Maastrichtian–Paleocene period of Andean tectonic loading was followed by an unloading stage during the Early–Middle Eocene (Roddaz et al. 2010). From the Middle–Late Eocene, the Amazonian retroarc foreland basin was subjected to continuous flexural subsidence driven by the continuous Andean tectonic loading, which promoted high sedimentation rates in the foredeep depozone (Roddaz et al. 2010). The formation and forward propagation of the eastern Amazonian orogenic thrust wedge began in the Oligocene (30–24 Ma) (Eude et al. 2015), causing flexural subsidence and high sedimentation rates in the Marañon foredeep (Roddaz et al. 2010).

The stratigraphy of Amazonian foreland basins has been synthesized by Roddaz et al. (2010). The Neogene sedimentary pile consists of late Oligocene–Miocene Chambira, Early–Late Miocene Pebas, Pliocene Marañon, and Quaternary Corrientes formations. These units are generally poorly dated. The Pebas Formation, with a thickness of approximately 1000 m (Wesselingh et al. 2006a), transitionally overlies the Chambira Formation (Oligocene) and is in underlying concordant contact with the Marañon Formation. The transition is characterized by blue clays, fine-grained lithic sandstones, and lignite layers rich in diverse and well-preserved invertebrate and vertebrate fossils; the base of this formation was dated around 22.5–23.9 Ma (Oligocene–Miocene boundary) (Wesselingh et al. 2006a).

3. Previous studies

Numerous studies have recorded the presence of palynomorph taxa in the Pebas and Solimões formations and other coeval units outcropping in Colombia, Brazil, and Peru (Hoorn 1993, 1994a, 1994b, 2006; Hoorn et al. 1995, 1996, 2010a, 2010b; Räsänen et al. 1995; Gingras et al. 2002a, 2002b; Hoorn and Ramos Feijó 2006; Rebata et al. 2006a, 2006b; Wesselingh 2006; Wesselingh et al. 2006a, 2006b, 2010; Hovikoski et al. 2007b; Latrubesse et al. 2007, 2010; da Silva et al. 2010; Gross et al. 2011; Leite et al. 2017; Leandro et al. 2019; Linhares et al. 2019). These formations generally date from the Early–Late Miocene (Hoorn and Wesselingh 2010; Latrubesse et al. 2010; Roddaz et al. 2010; Boonstra et al. 2015; Hoorn et al. 2017; Jaramillo et al. 2017; Leite et al. 2017). However, it is important to note that no palynological studies exist that deal with the Neogene sedimentary units of the Marañon Basin.

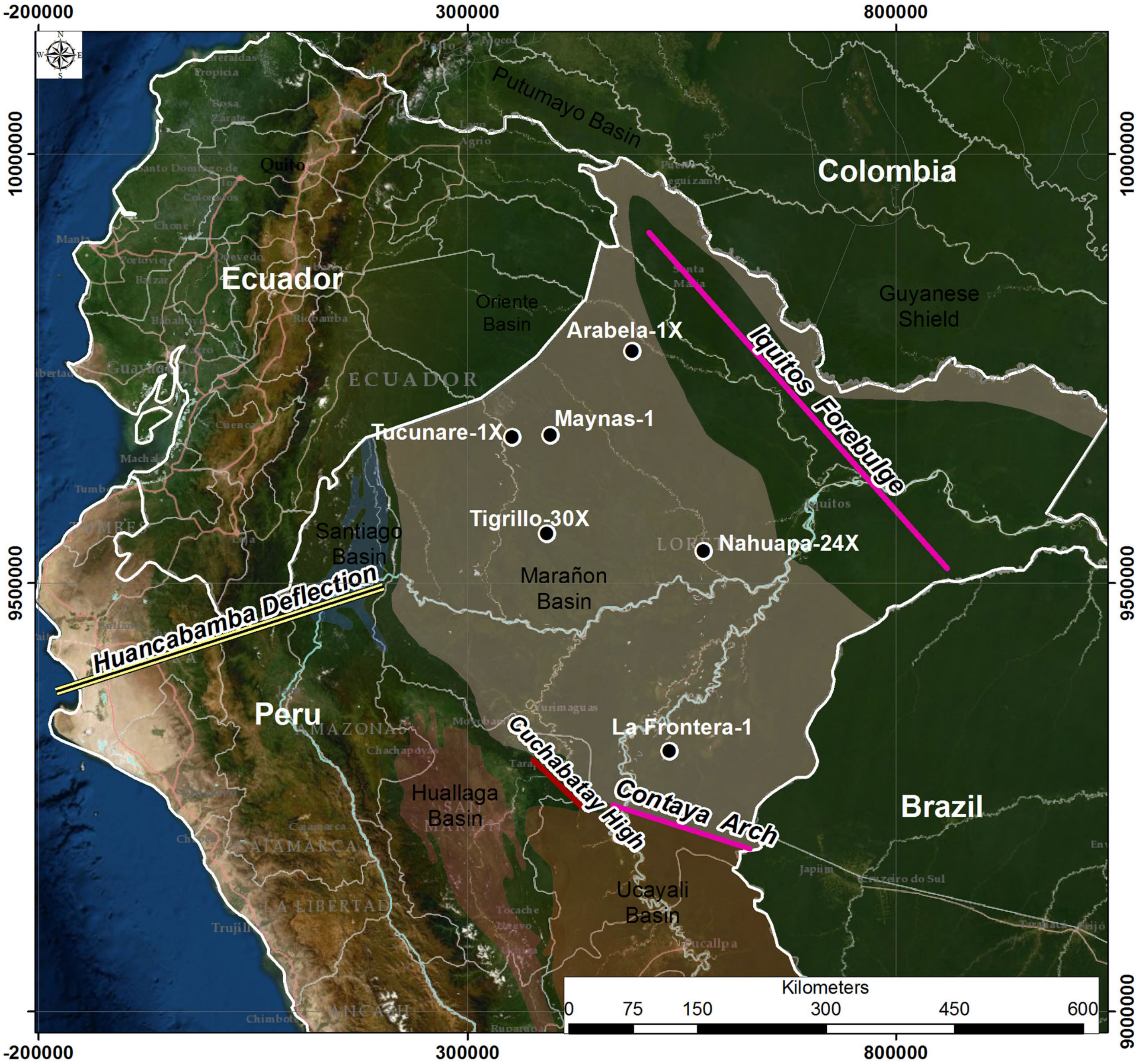

Figure 1. Location of the six studied deep exploration wells (white-black circles). Structural boundaries of the Marañon Basin (after Roddaz et al. 2005).

Neogene deposits of the Marañon Basin, to date, have been dated mainly based on palynozones defined by Hoorn (1993) for the Solimões and Acre basins, the Malacostraca zones defined by Wesselingh et al. (2006a), and the ostracod zones defined by Muñoz-Torres et al. (2006). Hoorn (1993) defined five palynozones for the Solimões Basin: the *Verrutricolporites* Acme Zone (Early Miocene), the *Retitricolporites* Acme Zone (Early Miocene), the *Psiladiporites–Crototricolpites* Concurrent Range Zone (late Early to early Middle Miocene), the *Crassoretitriletes* Interval Zone (Middle Miocene), and the *Grimsdalea* Interval Zone (late Middle to early Late Miocene), which correlated with those by Germeraad et al. (1968) and Lorente (1986). In the same basin, da Silva et al. (2010) defined the Asteraceae–*Fenestrites* Zone and recognized the *Psilatricolporites caribbiensis* palynozone of Lorente (1986). More recently, these zones in the Solimões Basin were recognized by (Leite et al. 2017; Linhares et al. 2017, 2019; Leandro et al. 2019), who further identified Lorente's (1986) palynozones: the *Crassoretitriletes* Interval Zone (Middle Miocene), the Asteraceae Interval Zone (Late Miocene), the *Psilatricolporites caribbiensis* Interval Subzone (latest Miocene–Pliocene), and the *Echitricolporites–Alnipollenites* Interval Subzone (Late Pliocene).

4. Sample material and procedures

A total of 77 ditch-cutting samples from six exploration wells (Arabela-1X, Maynas-1, Tucunare-1X, Tigrillo-30X, Nahuapa-24X, and La Frontera-1) located in the Marañon Basin were studied for their palynological content (Table 2 and Figure 1). The samples varied from silty shale to shale, claystone, sandy clay, and clayey, very fine sandstone. The palynological samples were prepared according to the

Table 2. Analyzed intervals [depth in feet (1 ft = 0.3 meters)] from Arabela-1X, Maynas-1, Tucunare-1X, Tigrillo-30X, Nahuapa-24X, and La Frontera-1 wells in the Marañon Basin and Centro de Investigaciones Científicas y Transferencia de Tecnología a la Producción (CICYTTP-PI) collection number of each analyzed sample.

Well	CICYTTP	Depth	Well	CICYTTP	Depth	Well	CICYTTP	Depth
Arabela1X	2005	186 – 195	Tigrillo-30X	2036	1618 – 1628	Nahuapa-24X	2052	674 – 683
	2006	250 – 259		2037	1728 – 1737		2053	701 – 710
	2007	277 – 286		2038	1820 – 1829		2054	738 – 747
	2008	341 – 351		2039	1966 – 1975		2055	783 – 792
	2009	360 – 369		2040	2094 – 2103		2056	856 – 866
	2010	369 – 378		2041	2112 – 2121		2057	948 – 957
	2011	451 – 460		2042	2130 – 2140		2058	1021 – 1030
	2012	497 – 506		2043	2231 – 2240		2059	1085 – 1094
	2013	543 – 552		2044	2322 – 2332		2060	1103 – 1112
	2014	552 – 561		2045	2432 – 2441		2061	1140 – 1149
	2015	689 – 698		2046	2551 – 2560		2062	1195 – 1204
	2016	872 – 881		2047	2652 – 2661		2063	1341 – 1350
	2017	1009 – 1018		2048	2770 – 2780		2064	1405 – 1414
Maynas-1	2018	823 – 838		2049	2917 – 2926		2065	1496 – 1506
	2019	1021 – 1036		2050	3054 – 3063		2066	1588 – 1597
	2020	1341 – 1356		2051	3246 – 3255		2067	1698 – 1707
	2021	1600 – 1615					2068	1743 – 1753
	2022	1859 – 1874					2069	1753 – 1762
	2023	2164 – 2179					2070	1798 – 1807
	2024	2438 – 2447					2071	1890 – 1899
Tucunare-1X	2025	1524 – 1539				La Frontera-1	2072	360 – 366
	2026	1631 – 1646					2073	469 – 475
	2027	1676 – 1692					2074	567 – 573
	2028	1768 – 1783					2075	579 – 585
	2029	1798 – 1813					2076	671 – 677
	2030	1951 – 1966					2077	823 – 829
	2031	2057 – 2073					2078	945 – 951
	2032	2133 – 2149					2079	975 – 981
	2033	2194 – 2210					2080	1250 – 1256
	2034	2240 – 2255					2081	1341 – 1347
	2035	2316 – 2332						

CICYTTP: Centro de Investigaciones Científicas y Transferencia de Tecnología a la Producción

Slides collection number in CICYTTP:
CICYTTP-2005 to CICYTTP-2081

Depth: analyzed intervals of each well in meters

standard procedure (Wood et al. 1996). The preparation of palynological slides was carried out in the Paleosedes Laboratory in Bogotá, Colombia (http://www.paleosedes.tk). Samples were processed using hydrochloric acid, hydrofluoric acid, and zinc chloride solutions. The slides were analyzed at the Paleosedes Biostratigraphy Laboratory and the Palynostratigraphy and Paleobotany Laboratory of the institute CICYTTP-CONICET-ER-UADER (http://www.cicyttp.org.ar) in Argentina. Slides and residues are housed at the Palynostratigraphy and Paleobotany Laboratory of the Centro de Investigaciones Científicas y Transferencia de Tecnología a la Producción (CICYTTP) and cataloged under CICYTTP acronyms; Table 2).

Two slides per sample (oxidized and non-oxidized) were scanned for palynomorph identification using transmitted light microscopes with a digital camera (Leitz Labor Lux S and Labomed 10 in Colombia; Nikon E200 and Labomed 5 in Argentina). Well-preserved specimens were selected and illustrated in Plate 1 using England Finder™ coordinates. Palynomorph counting and logging were done by applying straight transects across each slide. Species names and abundance of taxa were recorded on data sheets. Six palynomorph distribution charts were prepared based on each palynomorph identified in the well sections, and the abundances of spores, pollen grains, fungal spores, algae, dinoflagellate cysts, acritarchs, foraminiferal linings, and copepod eggs were tabulated in the Tilia software (Grimm 2015) (Appendices 1–6). The recovered palynomorphs were gathered in seven morphogroups (Table 3) and percentages for the morphogroups in all wells were calculated (Table 4). Approximately 100–200 specimens were counted per sample. However, some samples with abundances lower than 100 identifications were also included in the qualitative analyses due to their biostratigraphic significance (see Appendices 1–6).

The qualitative vertical arrangement of taxa identified from the wells was used to interpret first downhole occurrence or last appearance datum (LAD) and last downhole occurrence or first appearance datum (FAD) data. Palynostratigraphic studies and online catalogues of species from northern South America (Van der Hammen 1956; Germeraad et al. 1968; Regali et al. 1974a, 1974b; Lorente 1986; Muller et al. 1987; Tryon and Lugardon 1991; Hoorn 1993, 1994a; da Silva et al. 2010; Jaramillo et al. 2011; Raine et al. 2011; Silveira and Souza 2015, 2016; Leite et al. 2017; Williams et al. 2017; Jaramillo and Rueda 2019) were consulted for taxonomic determinations (see the list of species with their authors below) and stratigraphic ranges of the species suitable for biostratigraphy (Table 5). Critical palynomorph taxa were selected according to their stratigraphic value, and the most biostratigraphically significant events are indicated in Figure 2. To validate these findings, the graphic correlation technique of Shaw (1964) was applied to the dataset using GraphCor: Interactive Graphic Correlation software (Hood 1998) to obtain a composite section (Table 6) that was reordered and plotted (Figure 3) according to the stratigraphic succession, thus revealing biostratigraphic units. Details of this method can be consulted in the extensive compilation of Mann and Lane (1995).

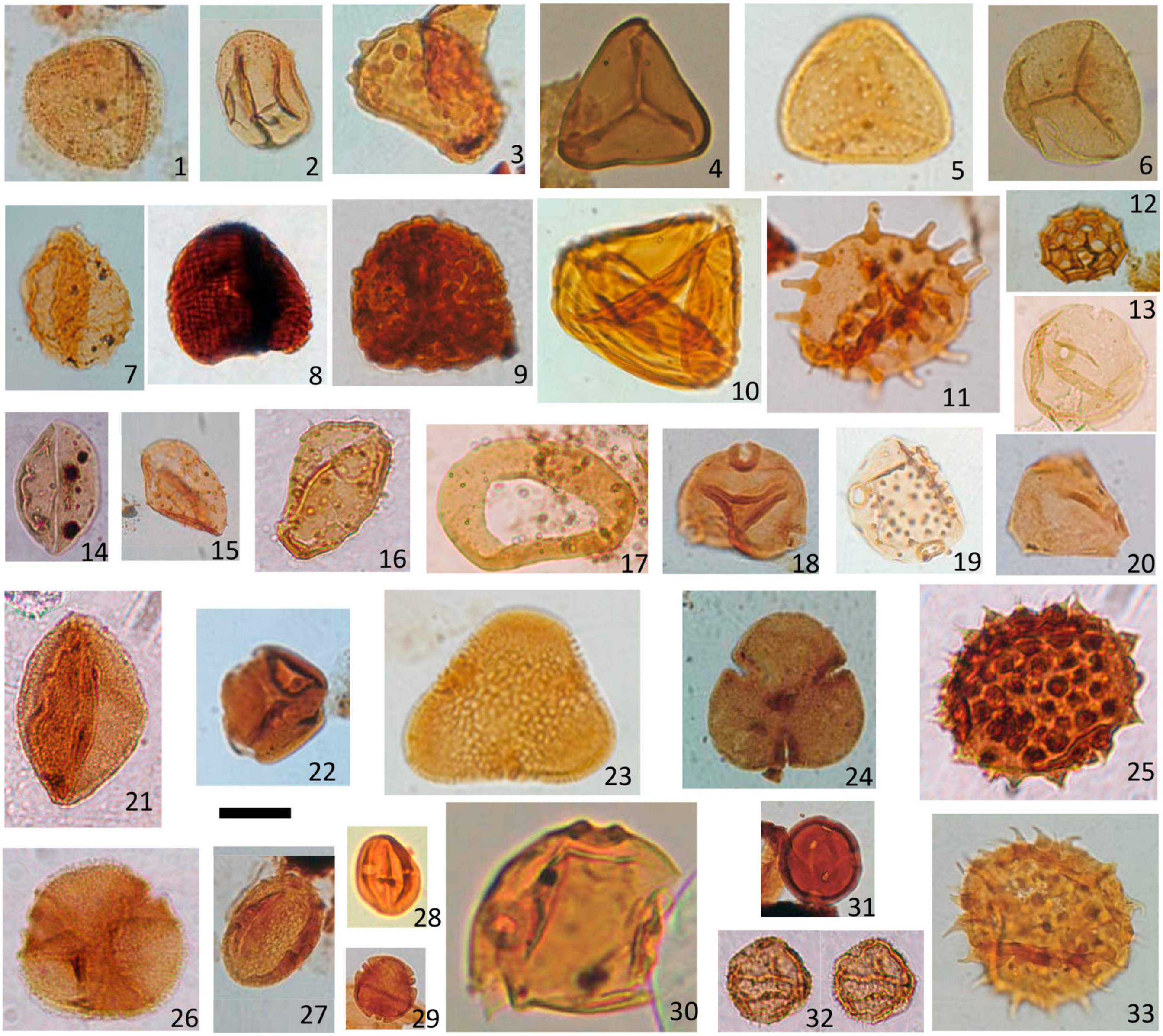

Plate 1. Photographs of the main palynomorphs from the studied wells. 1. *Laevigatosporites catanejensis* CICYTTP-2005 Arabela 1X (610–640ft), EF M12/2; 2. *Laevigatosporites granulatus* CICYTTP-2014 Arabela 1X (1810–1840ft), EF L32/2-4; 3. *Polypodiisporites usmensis* CICYTTP-2007 Arabela 1X (910–940ft), EF H25/2; 4. *Cyathidites congoensis* CICYTTP-2074 Frontera 1 (1860–1880ft), EF N35/2; 5. *Foveotriletes ornatus* CICYTTP-2068 Nahuapa 24X (5720–5750ft), EF N32/1-2; 6. *Osmundacidites ciliatus* CICYTTP-2074 Frontera 1 (1860–1880ft), EF R35/1; 7. *Retitriletes altimuratus* CICYTTP-2061 Nahuapa 24X (3740–3770ft), EF W21/3-4; 8. *Cicatricosisporites dorogensis* CICYTTP-2017 Arabela 1X (3310–3340ft), EF E3/3-2; 9. *Crassoretitriletes vanraadshooveni* CICYTTP-2052 Nahuapa 24X (2210–2240ft), EF H43/1; 10. *Magnastriatites grandiosus* CICYTTP-2057 Nahuapa 24X (3110–3140ft), EF O43/2; 11. *Grimsdalea magnaclavata* CICYTTP-2053 Nahuapa 24X (2300–2330ft), EF W17/3; 12. *Gomphrenipollis minimus* CICYTTP-2061 Nahuapa 24X (3740–3770ft), EF T34/2-3; 13. *Monoporopollenites annulatus* CICYTTP-2058 Maynas 1 (3350–3400ft), EF P44/1; 14. *Psilamonocolpites medius* CICYTTP- 2046 Tigrillo 30X (8370–8400ft), EF Q11/4; 15. *Mauritiidites franciscoi minutus* CICYTTP-2014 Arabela 1X (1810–1840ft), EF S38/1; 16. *Mauritiidites franciscoi franciscoi* CICYTTP-2031 Tucunare 1X (6750–6800ft), EF H42/1; 17. *Cyclusphaera scabrata* CICYTTP-2020 Maynas 1 (4400–4450ft), EF E10/3; 18. *Corsinipollenites psilatus* CICYTTP-2014 Arabela 1X (1810–1840ft), EF N12; 19. *Echitriporites cricotriporatiformis* CICYTTP-2006 Arabela 1X (820–850ft), EF F44/3; 20. *Proteacidites triangulatus* CICYTTP-2061 Nahuapa 24X (3740–3770ft), EF Z33/1; 21. *Retitricolpites simplex* CICYTTP-2035 Tucunare 1X (7600–7650ft), EF P43/2; 22. *Crassiectoapertites columbianus* CICYTTP-2061 Nahuapa 24X (3740–3770ft), EF F38/1; 23. *Bombacacidites nacimientoensis* CICYTTP-2059 Nahuapa 24X (3560–3590ft), EF J35/1-3; 24. *Bombacacidites brevis* CICYTTP-2017 Arabela 1X (3310–3340ft), EF R40/3; 25. *Malvacipolloides maristellae* CICYTTP-2034 Tucunare 1X (7350–7400ft), EF N25/2; 26. *Margocolporites vanwijhei* CICYTTP-2046 Tigrillo 30X (8370–8400ft), EF M23/4; 27. *Rhoipites guianensis* CICYTTP-2014 Arabela 1X (1810–1840ft), EF H35/1; 28. *Siltaria hammenii* CICYTTP-2072 Frontera 1 (1180–1200ft), EF X48; 29. *Ranunculacidites operculatus* CICYTTP-2007 Arabela 1X (910–940ft), EF G23/3; 30. *Psilastephanoporites tesseroporus* CICYTTP-2077 Frontera 1 (2700–2720 ft), EF W34/3; 31. *Perisyncolporites pokornyi* CICYTTP-2011 Arabela 1X (1480–1510ft), EF V37/3; 32. *Echiperiporites akanthos* CICYTTP-2027 Tucunare 1X (5500–5550ft), EF U27/2; left high focus and right lowfocus; 33. *Echiperiporites estelae* CICYTTP-2016 Arabela 1X (2860-2890ft), EF G23/1. Scale bar is 20 μm for all pictures except for Figures 9 and 10 where it represents 30 μm.

5. General characterization of the palynofloral assemblages

Seventy-seven samples from the Arabela-1X, Maynas-1, Tucunare-1X, Tigrillo-30X, Nahuapa-24X, and La Frontera-1 wells in the Marañon Basin (Table 2; Figure 1) yielded 6262 identifiable grains, as summarized in Table 3. Quantitative distribution of palynomorphs in the wells (Table 3 and 4; Appendices 1–6) reveals a total of 226 morphotypes, including 80 genera and 150 species of pollen grains, 24 genera and 43 species of spores, nine genera and eight species of dinoflagellate cysts, five genera of algae, four morphotypes, and two

Table 3. Total grains counted per each analyzed well and percentage of each morphogroup from Arabela-1X, Maynas-1, Tucunare-1X, Tigrillo-30X, Nahuapa-24X, and La Frontera-1 wells in the Marañon Basin. NA: not applicable.

Morphogroups	Total grains	% of 6262 grains	Morphotypes	Genera	Species
Spores	3232	51.6	44	24	43
Pollen grains	1478	23.6	152	80	150
Fungal spores	167	2.7	4	2	NA
Algae	899	14.4	7	5	NA
Dinoflagellate cysts	243	3.9	13	9	8
Foram linings	110	1.8	5	NA	NA
Copepod eggs	133	2.1	1	NA	NA
Total	6262	100.00	226	120	201

Table 4. Total grains counted per morphogroup in each analyzed well and percentage of each morphogroup from Arabela-1X, Maynas-1, Tucunare-1X, Tigrillo-30X, Nahuapa-24X, and La Frontera-1 wells in the Marañon Basin.

Morphogroups	Arabela-1X	Maynas-1	Tucunare-1X	Tigrillo-30X	Nahuapa-24X	La Frontera-1
Spores	46.8	65.3	49.7	64.7	48.5	22.8
Pollen grains	28.5	16.5	28.5	24.6	19.1	25.6
Fungal spores	3.3	0.5	0.3	1.7	3.9	7.1
Algae	13.4	6.0	11.8	5.5	25.7	24.4
Dinoflagellate cysts	6.6	0.9	3.5	1.8	1.0	14.5
Foram linings	1.1	4.4	0.0	1.7	0.4	5.6
Copepod eggs	0.2	6.4	6.1	0.0	1.3	0.0
Total specimens	2120	1176	593	654	1395	324

genera of fungal spores. Foraminiferal linings and copepod eggs (indeterminate copepods) were also identified. Of the identified palynomorphs, 75.1% belonged to pollen and spore groups, 14.3% were algae, and 7.8% included dinoflagellate cysts, acritarchs, foraminiferal linings, and other palynomorph remains. Fungal palynomorphs (2.8%) and abundant organic matter were recovered in all the samples.

Fairly well-preserved pteridophyte–bryophyte spores, angiosperm and gymnosperm pollen grains, phytoplankton (chlorophyceans, acritarchs, and dinoflagellate cysts) and miscellaneous groups (foraminifera, copepods, and fungal remains), characterize the palynoflora obtained from the six wells. The first group was mainly composed of spores such as *Azolla*, *Cicatricosisporites*, *Crassoretitriletes*, *Cyathidites*, *Deltoidospora*, *Echinatisporis*, *Foveotriletes*, *Laevigatosporites*, *Magnastriatites*, *Polypodiisporites*, *Psilatriletes*, *Striatriletes*, and *Verrucosisporites*–*Verrutriletes*.

Angiosperm pollen grains were frequent and more diverse, including *Bombacacidites*, *Corsinipollenites*, *Crassiectoapertites*, *Cyclusphaera*, *Echiperiporites*, *Echipollenites*, *Echitriporites*, *Inaperturopollenites*, *Ladakhipollenites*, *Malvacipolloides*, *Mauritiidites*, *Paleosantalaceaepites*, *Perfotricolpites*, *Perisyncolporites*, *Proxapertites*, *Proteacidites*, *Psilamonocolpites*, *Psilastephanocolporites*, *Psilatricolporites*, *Retimonocolpites*, *Retipollenites*, *Retistephanoporites*, *Retitrescolpites*, *Retitricolpites*, *Retitricolporites*, *Scabrapollenites*, *Siltaria*, *Spinizonocolpites*, and *Striatopollis*.

Gymnosperm pollen grains were rare and less diverse: *Araucariacites*, *Cyclusphaera*, *Inaperturopollenites*, *Podocarpidites*, and *Striapollenites*. Chlorophycean algae such as *Botryococcus*, *Oedogonium*, *Pediastrum*, and *Pterospermella* were obtained. Other phytoplankton, including acritarchs and dinoflagellate cysts, such as *Apteodinium*, *Batiacasphaera*, *Bosedinia*, aff. *Ceratium*, *Cribroperidinium*, *Leiosphaeridia*, *Quadrina*, *Selenopemphix* spp., and *Operculodinium* and *Polysphaeridium* groups, were common and always accompanied by foraminiferal linings, copepod eggs, and fungal palynomorphs, such as *Fusiformisporites*, Microthyraceae, and *Tetraploa*. The distribution of the palynomorphs in the above-mentioned wells, their relative abundances (range charts), and extended Tilia diagrams are shown in Appendices 1–6, and key markers are illustrated in Plate 1.

6. Definition of palynozones

Fifty-two biostratigraphic marker species were recognized in the six boreholes (Table 5). Some occurred in all the wells, whereas others did not (Appendices 1–6), but all have a wide geographic distribution and well-known stratigraphic ranges given as FADs and LADs in millions of years ago for each taxon and/or based on stratigraphic ranges that have been used in biostratigraphic definitions in northern South America (Lorente 1986; Muller et al. 1987; Hoorn 1993; da Silva et al. 2010; Jaramillo et al. 2011) and elsewhere (Bujak and Williams 1985; Macphail 1999; Williams et al. 2017). Therefore, they are useful for dating the studied successions in this basin and for proposing regional correlations. Six palynozones named from the oldest to the youngest, namely Mar-A to Mar-F (‘Mar’ is the abbreviation for ‘Marañon’) are proposed considering the vertical distribution of the taxa (Figures 2–4; Appendices 1–6) based on the analysis of qualitative biostratigraphic events. A quantitative deterministic method of graphic correlation (Shaw 1964) in order to test this scheme was run in GraphCor: Interactive Correlation Software Hood (1998). Maximum stratigraphic ranges of species from previously known appearances and disappearances in each well (Table 6) allowed the construction of a biostratigraphic ordination in a composite section (Figure 3) according to last appearances of species. This method corroborates the proposed zonation based on a qualitative analysis, also evidenced by stratigraphically constrained cluster analysis (CONISS) in the Tilia software (Grimm, 2015) for each well

Table 5. Marker age of palynomorphs recovered in the Arabela-1X, Maynas-1, Tucunare-1X, Tigrillo-30X, Nahuapa-24X, and La Frontera-1 boreholes in the in the Marañon Basin, in alphabetical order (occurrence levels are included; depth in meters). (1) da Silva-Caminha et al. (2010), (2) González-Guzmán (1968), (3) Hoorn (1993), (4) Jaramillo et al. (2011), (5) Eisawi and Schrank (2008), (6) Cole (1992); (7) De Verteuil et al. (1992), (8) Raine et al. (2011) and (9) Williams et al. (2017).

MARKER SPECIES	FAD		LAD	ARABELA-1X	MAYNAS-1	TUCUNARE-1X	TIGRILLO-30X	NAHUAPA-24X	LA FRONTERA-1
Acaciapollenites myriosporites (1)(8)	Neogene	–	Neogene						1341-1347
Apteodinium australiense (9)	Early Eocene	–	Midle Miocene/ Serravalian						1250-1256
Bombacacidites araracuarensis(3)	Early Miocene	–	early Middle Miocene			1524-1539			
Bombacacidites gonzalezii (4)	51.49	–	19.7		2164-2179				
Bombacacidites nacimientoensis (4)	56.85	–	13.05				1618-2103	674-1094	
Bosedinia infragranulata (6)	Late Oligocene	–	Miocene						579-585
Cicatricosisporites dorogensis (4)	48.61	–	23.03	1009-1018	2621-2630	2316-2332	3356-3365	2054-2060	
Cistacearumpollenites rotundiporus(1)	Neogene	–	Neogene						360-366
Corsinipollenites oculusnoctis (1)	Early Miocene	–	Middle Miocene		1859-2447	1798-2149			671-677
Corsinipollenites collaris (1)	Miocene	–	Early Plioc					1798-1807	
Corsinipollenites psilatus (4)		–	17.33	451-460	1341-1356	1676-1692		674-2054	
Crototricolpites annemariae (4)	52.49	–	13						975-981
Crassoretitriletes vanraadshooveni (4)	14.18	–	3.4					674-683	360-366
Ctenolophinidites suigeneris (1)	Miocene	–	Early Plioc					1140-1506	579-585
Cyathidites congoensis (5)	Late Miocene	–	Pliocene	186-1009	1021-2447	1524-2332	3255-1618	674-1753	567-573
Cyclusphaera scabrata (4)	55.8	–	16.92	360-881	1341-1356				
Echitriporites cricotriporatiformis (4)	16.8	–	3.94	250-259					
Echiperiporites lophatus (1)	Miocene	–	Early Plioc					701-710	
Foveotricolporites lenticuloides (1)	Neogene	–	Neogene						579-585
Gomphrenipollis minimus (1)	Miocene	–	Early Plioc					1140-1149	
Grimsdalea magnaclavata(4)	16.09	–	3.4					701-792	
Ladakhipollenites simplex(4)	59.92	–	12.87	250-506	1021-1356				
Ladakhipollenites? caribbiensis (1)	Late Miocene	–	Pliocene						567-573
Laevigatosporites catanegensis (4)	42.53	–	4.32	186-195					
Lanagiopolllis crassa (4)	51.3	–	4.7						567-573
Magnaperiporites spinosus(4)	31.96	–	12.98	552-561					
Malvacipolloides maristellae (4)	17.71	–	0.39	186-506	1021-1356	1524-2332	2130-2240	1021-1350	823-981
Mauritiidites crassibaculatus(4)		–	11.85		823-2164		1758-2917		
Multiporopollenites apauciporatus(4)		–	23		2438-2447				
Nijssenosporites fossulatus(4)	19.05	–	1.03						579-585
Osmundacidites ciliatus (5)	Late Miocene	–	Pliocene						567-573
Palaeosantalaceaepites cingulatus (4)	12.08	–	3.72					674-683	567-573
Psilastephanoporites tesseroporus (4)	13.9	–	5.48	250-259					
Quadrina? condita (7)	Middle Miocene	–	Late Miocene						579-585
Retimonocolpites maximus (3)	Miocene	–	Miocene						469-475
Retipollenites crotonicolumellatus(4)	13.94	–	3.56				1820-1829		
Retistephanoporites angelicus (2)	56	–	16				1966-1975		
Retitricolporites wijmstrae (3)	23	–	16	360-1018	1021-1615		1975-3255		
Retitricolporites "cacerolensis" (4)			16.26			1631-1646			
Retitriletes altimuratus (1)	Miocene	–	Early Pliocene					674-1149	
Retitriporites dubiosus (4)	51.47		14.27	277-286					
Selenopemphis nephroides(4)	17.83	–	6.89	341-351					
Siltaria hammenii (1)	Neogene	–	Neogene						360-366
Siltaria santaisabelensis (1)	Miocene	–	Miocene						469-475

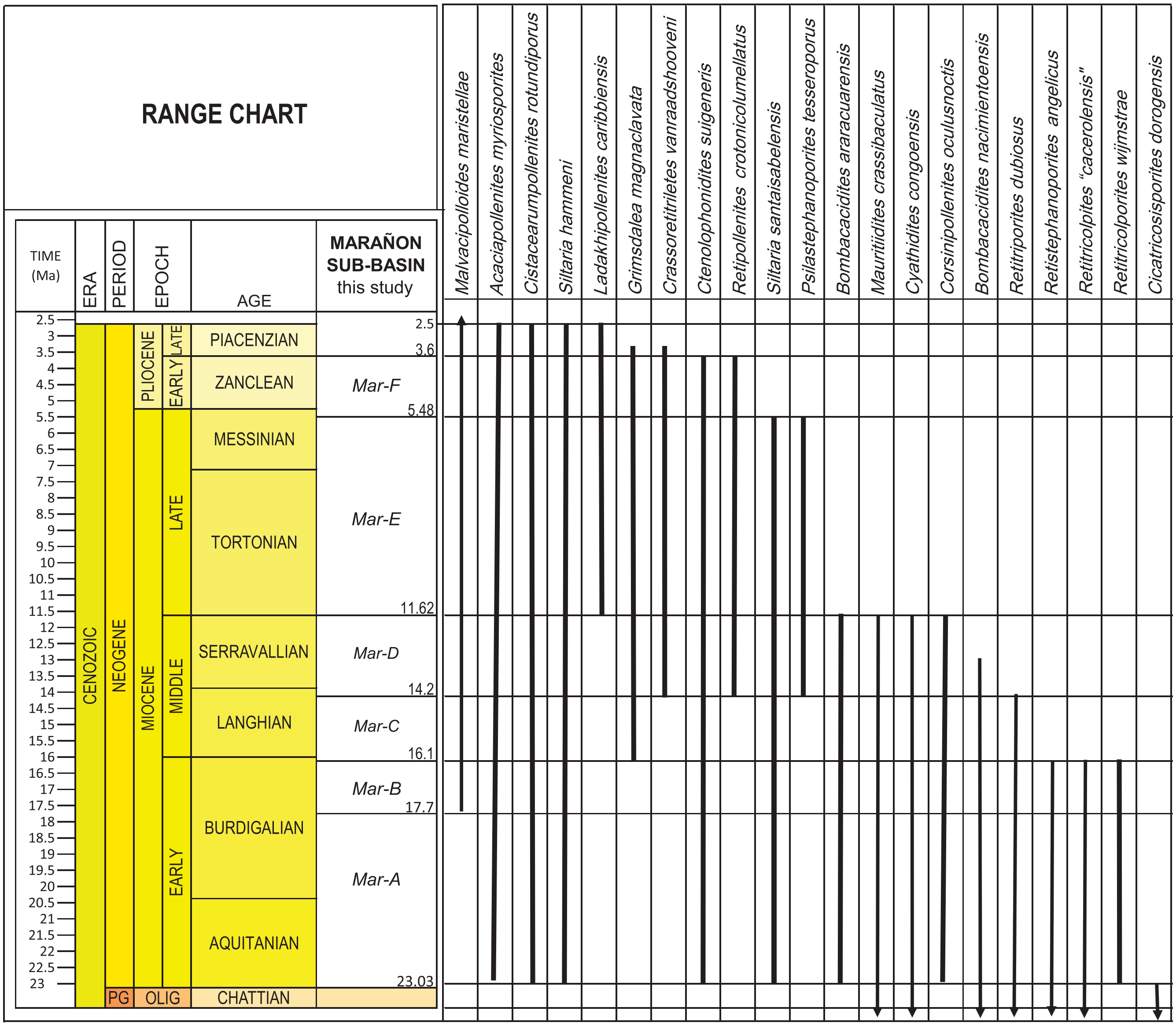

Figure 2. Range chart of taxa as used in this work, indicating the boundaries of the palynozones Mar-A to Mar-F.

(Appendices 1–6). The upper two zones are preliminarily characterized until further studies with more materials are carried out. The presence of well-known diagnostic species (FADs and LADs; Figures 2–4; Tables 5 and 6) supported the ages of the palynozones. In addition, seven timelines and a west–east and north–south correlation among the six wells were drawn (Figure 5), and a correlation of our palynozonation with other palynozones from northern South America (Figure 6) is also addressed below.

6.1. Mar-A Corsinipollenites oculusnoctis *Interval Zone*

Reference section. Arabela-1X interval 2890–1660 ft (881–506 m).

Distribution. This zone was recognized in all the wells: Arabela-1X interval 2890–1660 ft (881–506 m), Tigrillo-30X interval 10,680–7620 ft (3255–2323 m), Nahuapa-24X interval 4610–3230 ft (1405–985 m), Maynas-1 interval 8030–5250 ft (2438–1600 m), Tucunare-1X interval 7650–7400 ft (2332–2255.5 m) and La Frontera-1 interval 4420–4100 ft (1347–1250 m) (see Appendices 1–6 for details and Figures 2–6 for summary and correlation).

Description. We define the Mar-A *Corsinipollenites oculusnoctis* palynozone as occurring from the LAD of *Cicatricosisporites dorogensis* to the FAD of *Malvacipolloides maristellae* or, alternatively, it is from the FAD of Corsinipollenites oculusnoctis, the FAD of Retitricolporites wijmstrae, and/or the FAD of Acaciapollenites myriosporites to the FAD of Malvacipolloides maristellae as occurring respectively in the Maynas-1, Tigrillo-30X, and La Frontera-1 wells, to the FAD of *Malvacipolloides maristellae.*

Age. Aquitanian to Early Burdigalian (23.03–17.71 Ma).

Characteristics. The presence of Paleogene taxa whose extinction occurred in the Neogene, such as *Bombacacidites nacimientoensis*, *Corsinipollenites psilatus*, *Magnastriatites grandiosus*, *Mauritiidites franciscoi* var. *franciscoi*, *Mauritiidites franciscoi* var. *minutus*, *Retitricolpites simplex*, and *Spirosyncolpites spiralis*, among others, is notable. This zone is characterized by the inception of other species, such as

Table 6. Maximum stratigraphic ranges of species among the studied wells, constructed in a composite section from previously known appearances and disappearances of species in each well obtained by means of graphic correlation.

Composite section for taxa from sections in studied wells							
Acaciapollenites	*myriosporites*	−1018	−194	*Mauritiidites*	*franciscoi franciscoi*	−693	−282
Apteodinium	*australiense*	−888	−888	*Mauritiidites*	*franciscoi minutus*	−795	−165
Araliaceae	*pollenitis*	−364	−364	*Monoporopollenites*	*annulatus*	−603	−191
Arecipites	*perfectus*	−194	−165	*Monocolpopollenites*	*ovatus*	−451	−451
Bombacacidites	*araracuarensis*	−190	−190	*Osmundacidites*	*ciliatus*	−191	−191
Bombacacidites	*brevis*	−1013	−1013	*Paleosantalaceaepites*	*cingulatus*	−191	−191
Bombacacidites	*gonzalezi*	−1013	−834	*Perfotricolpites*	*digitatus*	−709	−254
Bombacacidites	*nacimientoensis*	−1013	−186	*Perisyncolporites*	*pokornyi*	−834	−194
Bombacacidites	*psilatus*	−1013	−1013	*Polyadopollenites*	*mariae*	−644	−245
Bosedinia	*infragranulata*	−194	−194	*Polypodiisporites*	*specious*	−693	−282
Retitricolpites	*"cacerolensis"*	−308	−236	*Polypodiisporites*	*usmensis*	−834	−217
Cicatricosisporites	*dorogensis*	−1018	−1018	*Polypodiisporites*	*verrucatus*	−442	−364
Colombipollis	*tropicalis*	−547	−547	*Proteacidites*	*triangulatus*	−442	−442
Corsinipollenites	*collaris*	−835	−835	*Proxapertites*	*minutus*	−364	−364
Corsinipollenites	*oculusnoctis*	−945	−219	*Proxapertites*	*operculatus*	−547	−547
Corsinipollenites	*psilatus*	−556	−254	*Proxapertites*	*psilatus*	−364	−364
Crassiectoapertites	*columbianus*	−442	−442	*Proxapertites*	*verrucatus*	−364	−364
Crassoretitriletes	*vanraadshooveni*	−268	−195	*Psilamonocolpites*	*medius*	−644	−191
Ctenolophonidites	*suigeneris*	−612	−194	*Psilastephanocolporites*	*fissilis*	−834	−834
Cyathidites	*congoensis*	−795	−190	*Psilastephanoporites*	*tesseroporus*	−259	−165
Cyathidites	*minor*	−194	−191	*Psilatricolpites*	*papilioniformis*	−364	−364
Cyclusphaera	*scabrata*	−876	−364	*Psilatricolporites*	*crassoexinatus*	−364	−364
Deltoidospora	*adriennis*	−364	−191	*Psilatricolporites*	*operculatus minutus*	−364	−364
Echinatisporis	*muelleri*	−219	−219	*Quadrina?*	*condita*	−194	−194
Echiperiporites	*akanthos*	−945	−254	*Ranunculacidites*	*operculatus*	−282	−282
Echiperiporites	*estelae*	−876	−165	*Retimonocolpites*	*maximus*	−165	−165
Echiperiporites	*lophatus*	−217	−217	*Retimonocolpites*	*retifossulatus*	−945	−945
Echistephanoporites	*"annulatus"*	−193	−193	*Retipollenites*	*crotonicolumellatus*	−293	−288
Echitriporites	*cricotriporatiformis*	−254	−254	*Retistephanoporites*	*angelicus*	−363	−363
Foveotricolporites	*lenticuloides*	−194	−191	*Retistephanoporites*	*crassiannulatus*	−834	−256
Foveotriletes	*"ornatus"*	−795	−190	*Retitrescolpites*	*irregularis*	−680	−294
Foveotriletes	*proximopsilatus*	−245	−245	*Retitrescolpites*	*magnus*	−547	−364
Gomphrenipollis	*minimus*	−442	−442	*Retitrescolpites*	*saturum*	−963	−963
Grimsdalea	*magnaclavata*	−356	−217	*Retitrescolpites?*	*Irregularis*	−259	−194
Inaperturopollenites	*psilatus*	−364	−364	*Retitricolpites*	*colpiconstrictus*	−364	−364
Inaperturopollenites	*solimoensis*	−364	−364	*Retitricolpites*	*simplex*	−680	−193
Ladakhipollenites	*simplex*	−506	−250	*Retitricolporites*	*wijmstrae*	−1009	−363
Ladakhipollenites?	*caribbiensis*	−254	−191	*Retitriletes*	*altimuratus*	−442	−442
Laevigatosporites	*"annulatus"*	−497	−497	*Retitriporites*	*dubiosus*	−501	−282
Laevigatosporites	*catanegensis*	−190	−190	*Rhoipites*	*guianensis*	−556	−256
Laevigatosporites	*"gemmatus"*	−603	−603	*Rhoipites*	*hispidus*	−547	−191
Laevigatosporites	*granulatus*	−963	−236	*Selenopemphix*	*nephroides*	−346	−346
Laevigatosporites	*ovatus*	−194	−194	*Selenopemphix*	*quanta*	−194	−194
Magnaperiporites	*spinosus*	−556	−556	*Siltaria*	*santaisabelensis*	−165	−165
Magnastriatites	*grandiosus*	−835	−245	*Spirosyncolpites*	*spiralis*	−709	−364
Malvacipolloides	*maristellae*	−497	−409	*Striatriletes*	*saccolomoides*	−875	−447
Margocolporites	*vanwijhei*	−644	−556	*Tetracolporopollenites*	*maculosus*	−501	−346
Mauritiidites	*crassibaculatus*	−834	−245				

Apteodinium australiense, *Leiosphaeridia*, and *Polysphaeridium* groups (dinoflagellate cysts); the end of the acme of dinoflagellate cysts (Late Oligocene/Burdigalian); underlying *Malvacipolloides maristellae* (FAD); the first appearance of *Acaciapollenites myriosporites*, *Corsinipollenites collaris*, *Corsinipollenites oculusnoctis*, *Corsinipollenites psilatus*, *Ctenolophonidites suigeneris*, *Multiporopollenites* aff. *pauciporatus*/*M. pauciporatus*, *Cyathidites congoensis*, *Retitricolporites wijmstrae*, and *Selenopemphix nephroides* (dinoflagellate cysts); and the LAD of *Bombacacidites gonzalezii*. They frequently occur along with *Clavainaperturites* aff. *clavatus*, *Laevigatosporites* spp., *Polypodiisporites specious*, *Polypodiisporites* spp., and *Psilamonocolpites* spp., and seldom with *Magnaperiporites spinosus* (see Appendices 1–6 for details and Figures 2–6 for summary and correlations).

Comparison. The co-occurrence of several taxa (see Tables 5–6 and Figures 2–4) supports the correlation (summarized in Figure 6) of this zone with the palynostratigraphy of Venezuela (Lorente 1986), northern South America (Muller et al. 1987), and the Solimões Basin in Western Amazonia (Hoorn 1993). It is coeval with the T-12 *Horniella lunarensis* Zone from Llanos in Colombia (Jaramillo et al. 2011), the zonal boundaries of which are coeval with the Mar-A Zone. However, the T-12 taxon *Horniella lunarensis* is not present in the Mar-A *Corsinipollenites oculusnoctis* Zone (Figures 2–4)

6.2. Mar-B Malvacipolloides maristellae *Interval Zone*

Reference section. Arabela-1X 1660–1210 ft (506–369 m).

Distribution. This zone was recognized in the intermediate section of the six wells analyzed: Arabela-1X interval 1660–1180 ft (506–360 m), Maynas-1 interval 4450–3350 ft (1356–1021 m), Tucunare-1X interval 7400–5350 ft (2255.5–1631 m), Tigrillo 30X interval 7350–6450 ft (2240–1966 m), Nahuapa-24X interval 4430–2600 ft (1350–792 m), and La Frontera-1 interval

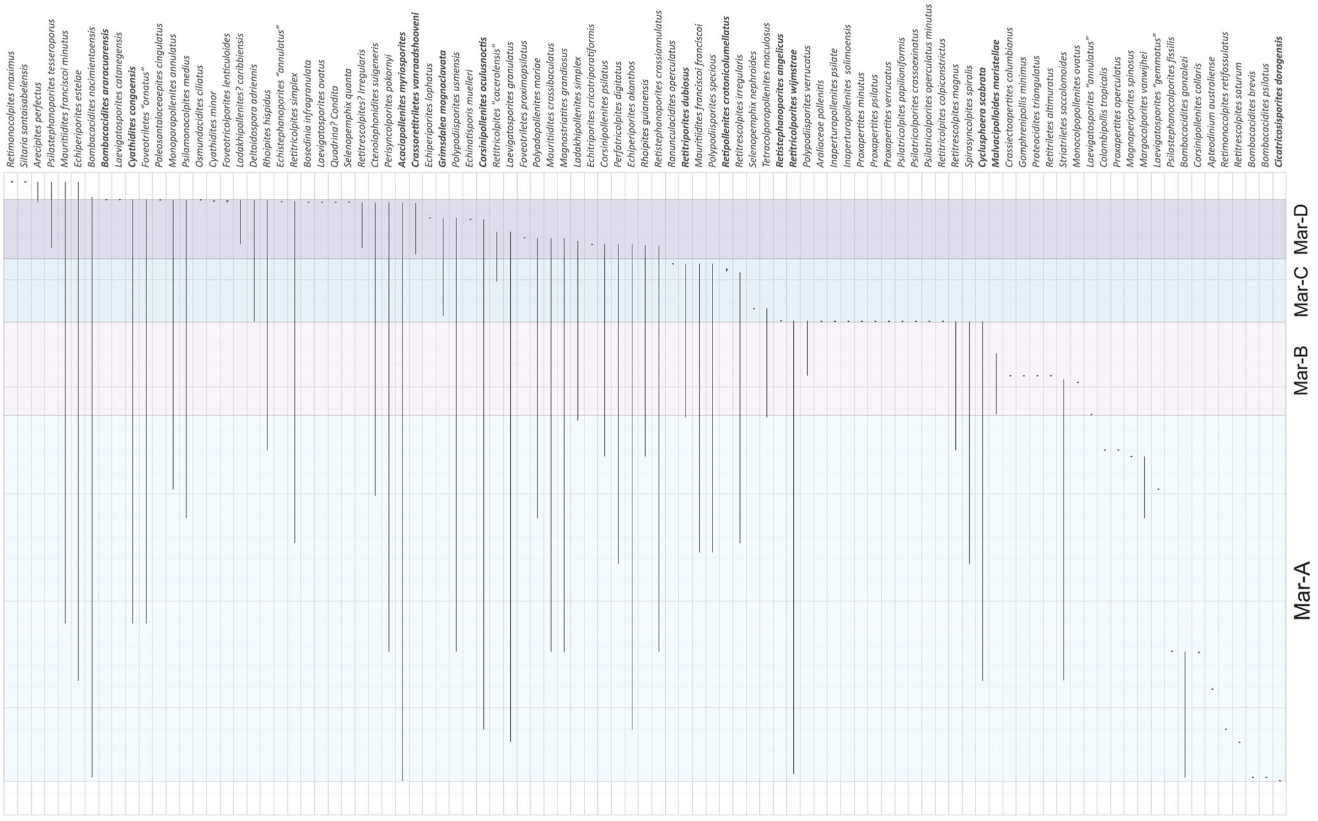

Figure 3. Maximum stratigraphic ranges of species ordered by last appearance datum (LAD) among the studied wells, constructed in a composite section from previously known appearances and disappearances of species in each well obtained by means of graphic correlation.

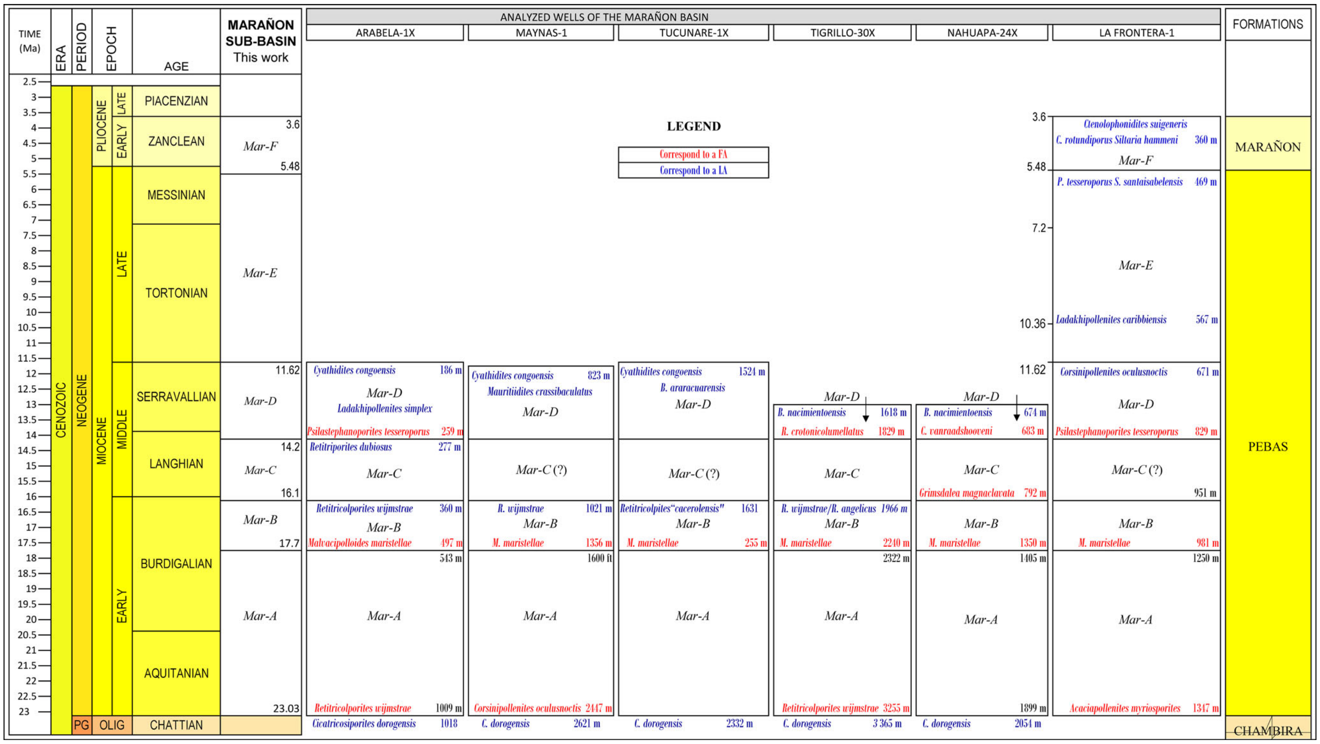

Figure 4. First palynological zonation for the Marañon Basin (this work) and correlation (time-lines). See Appendices 1–6 and Table 5 for details, and see Figures 2–3 and 5–6 for timeline correlation and correlation with other South American palynozones.

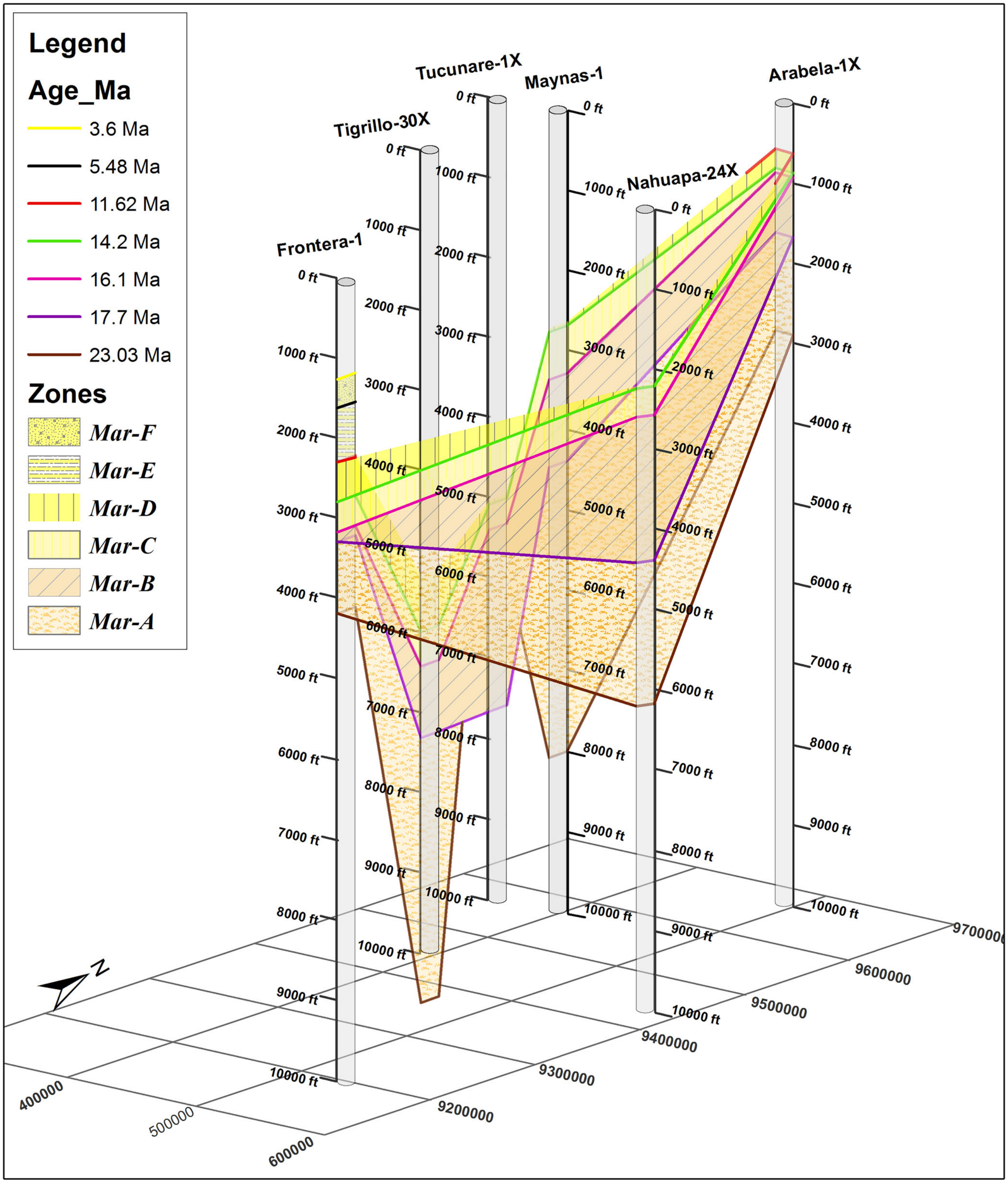

Figure 5. First palynological zonation for the Marañon Basin (this work), and south–west and north–east correlation and timelines between boreholes of the six exploration wells Arabela-1X, Maynas-1, Tucunare-1X, Tigrillo-30X, Nahuapa-24X, and La Frontera-1 in the Marañon Basin.

3220–3120 ft (981–951 m) (see Appendices 1–6 for details and Figures 2–6 for summary and correlation).

Description. We propose the Mar-B *Malvacipolloides maristellae* Zone as corresponding to the interval from the FAD of *Malvacipolloides maristellae* to the LAD of *Retitricolporites wijmstrae* and/or from the LADs of *Retistephanoporites angelicus* or *Cyclusphaera scabrata* to the FAD of *Grimsdalea magnaclavata* in the upper zone.

Age. Burdigalian (17.71–16.1 Ma).

Characteristics. This zone is characterized by the first appearance and continuous presence upward of *Malvacipolloides*

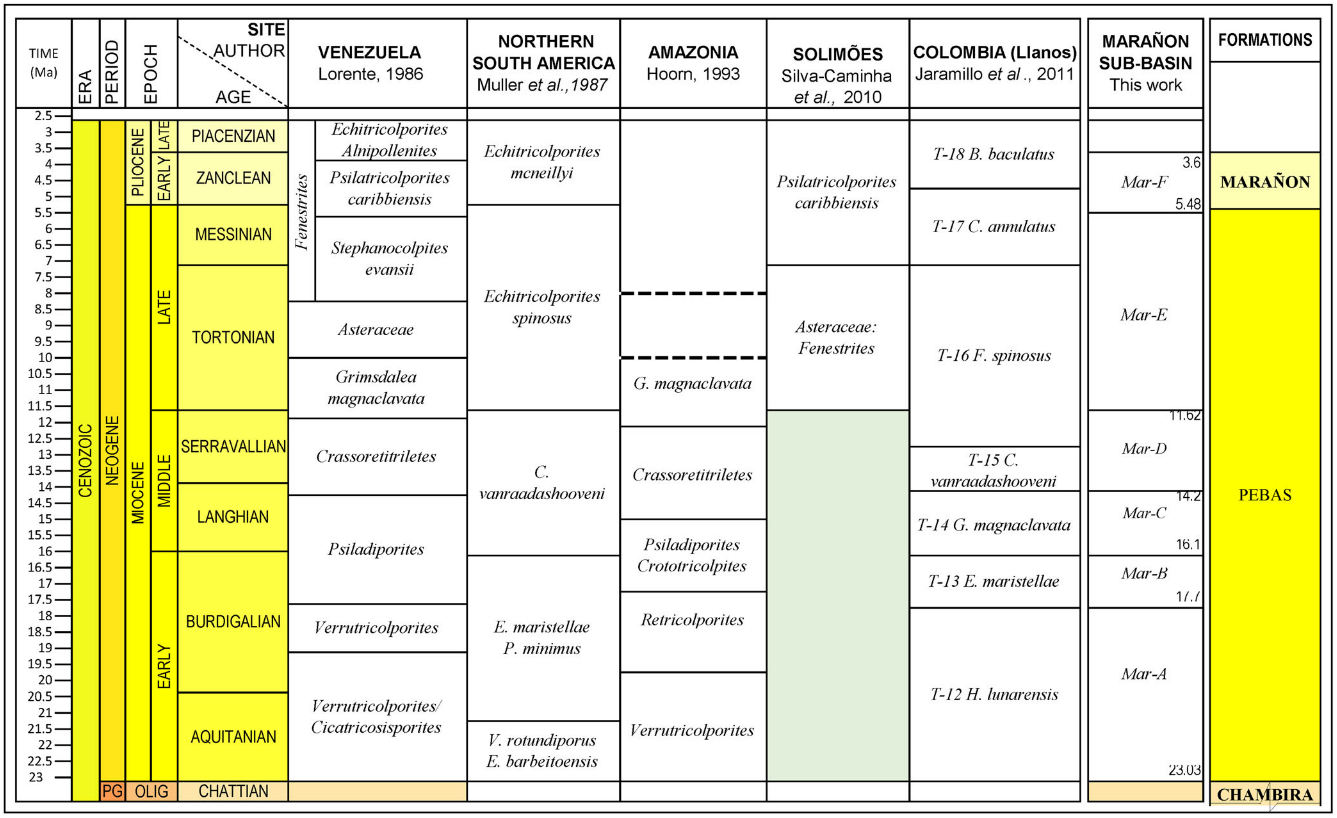

Figure 6. First palynological zonation for the Marañon Basin (this work) and its suggested correlation with other South American palynozones and the geological column.

maristellae, often accompanied by *Retistephanoporites angelicus*, *Corsinipollenites psilatus*, and *Retitricolporites wijmstrae*; the rare occurrence of *Bombacacidites nacimientoensis*, *Crototricolpites* cf. *annemariae*, *Ctenolophonidites suigeneris*, *Gomphrenipollis minima*, and *Retitriletes altimuratus*; and the continued presence of *Cyathidites congoensis*. Furthermore, *Clavainaperturites* aff. *clavatus*, *Laevigatosporites* spp., *Magnastriatites grandiosus*, *Mauritiidites franciscoi* var. *franciscoi*, *Mauritiidites franciscoi* var. *minutus*, *Perisyncolporites pokornyii*, *Polypodiisporites specious*, *Polypodiisporites* spp., *Polypodiisporites usmensis*, *Psilamonocolpites* spp., *Retipollenites* spp., and *Retitricolporites* sp. are commonly present in moderate abundances. Acritarchs and dinoflagellate cysts, such as *Batiacasphaera* sp., *Leiosphaeridia*, *Selenopemphix* spp., and *Operculodinium* group, also occur. A peak abundance of *Pterospermella* spp. (prasinophycean algae) is noticeable (see Appendices 1–6 for details and Figures 2–6 for summary and correlations).

Comparison. The co-occurrence of taxa (see Tables 5–6 and Figures 2–4 for details) supports the correlation of this zone with others in South America (summarized in Figure 5; Lorente 1986; Muller et al. 1987; Hoorn 1993; Jaramillo et al. 2011). The record of the Early Miocene *Malvacipolloides maristellae* (Muller et al. 1987) in the six wells (Figures 3 and 5) reinforces the age assigned to this zone. The zonal limits of the T-13 *Malvacipolloides maristellae* Zone from Llanos in Colombia (Jaramillo et al. 2011) were identified in one of the six wells, the Nahuapa-24X (Figure 3), supporting their correlation (Figures 4 and 5).

6.3. *Mar-C* Mauritiidites crassibaculatus *Assemblage Zone*

Reference sections. Arabela-1 interval 1180–910 ft (360–277 m) and Nahuapa-24X interval 2600–2240 ft (792–683 m).

Distribution. This zone was recognized in three wells, namely Arabela-1 interval 1180–910 (360–277 m), Tigrillo-30X interval 6450–6000 ft (1966–1829 m), and Nahuapa-24X interval 2600–2240 (792–683 m). Only the lower limit of this zone was recognized in the Maynas-1 and Tucunare-1X wells, and only the upper limit was recognized in the La Frontera-1 well (see Appendices 1–6 for details and Figures 2–6 for summary and correlations).

Description. The Mar-C *Mauritiidites crassibaculatus* Zone is defined as the interval with *Mauritiidites crassibaculatus* from the LAD of *Retitricolporites wijmstrae* (top of the lower zone) and/or the FADs of *Grimsdalea magnaclavata* to the LADs of *Retitriporites dubiosus* or FAD of *Crassoretitriletes vanraadshooveni* in the upper zone. Alternatively, the upper boundary may be defined by the FAD of *Psilastephanoporites tesseroporus* and/or that of *Retipollenites crotonicolumellatus* (in the upper zone), which should be used when *Retitriporites dubiosus* and *Crassoretitriletes vanraadshooveni* are absent.

Age. Latest Burdigalian to Late Langhian (16.1–14.2/13.9 Ma).

Characteristics. This zone is characterized by the continuous presence of *Ladakhipollenites simplex*, *Mauritiidites crassibaculatus*, *Bombacacidites nacimientoensis*, *Retitricolpites simplex* and *Cyathidites congoensis* along with the frequent occurrence of *Laevigatosporites* spp., *Magnastriatites grandiosus*, *Mauritiidites franciscoi* var. *franciscoi*, *Polypodiisporites* spp., *Polypodiisporites usmensis*, *Psilamonocolpites* spp., and *Retistephanoporites crassiannulatus*. It also contains *Leiosphaeridia* spp., *Selenopemphix* spp., *Selenopemphix nephroides*, and other indeterminate dinoflagellate cysts (see Appendices 1–6 for details and Figures 2–6 for summary and correlations).

Comparison. The co-occurrence of taxa (see Tables 5–6 and Figures 2–4 for details) supports the correlation of this zone with others in South America (summarized in Figure 5; Lorente 1986; Muller et al. 1987; Hoorn 1993; Jaramillo et al. 2011). This zone, in the six wells, is coeval with the T-14 *Grimsdalea magnaclavata* Zone (Figure 5) from Llanos in Colombia (Jaramillo et al. 2011). The T-14 Zone was defined as extending from the FAD of *G. magnaclavata* to the FAD of *Crassoretitriletes vanraadshooveni*. These zonal boundaries identified in Nahuapa-24X (Figure 4) reinforce the age given to our zone and their correlation (Figures 4–6).

6.4. Mar-D Crassoretitriletes vanraadshooveni *Assemblage Zone*

Reference section. Arabela-1 interval 850-610 ft (259–186 m) and La Frontera-1 interval 2720–2220 ft (829–677 m).

Distribution. This zone was recognized in the six wells analyzed: Arabela-1 interval 850–610 ft (259–186 m), Maynas-1 interval 2750–2700 (838–823 m), Tucunare-1X interval 5000–5050 (1524–1539 m), Tigrillo-30X interval 6000–5310 (1829–1618 m), Nahuapa-24X interval 2240–2210 ft (683–674 m), and La Frontera-1 interval 2720–2220 (829–677 m) (see Appendices 1–6 for details and Figures 2–6 for summary and correlations).

Description. The Mar-D *Crassoretitriletes vanraadshooveni* Zone is defined as the interval from the LADs of *Retitriporites dubiosus* (top of lower zone) and the FADs of the *Crassoretitriletes vanraadshooveni*, *Psilastephanoporites tesseroporus*, or *Retipollenites crotonicolumellatus* (which should be used when *Crassoretitriletes vanraadshooveni* and *Retitriporites dubiosus* are absent) to the LAD of *Corsinipollenites oculusnoctis* and/or the LAD of *Cyathidites congoensis*, and/or that of *Bombacacidites araracuensis*.

Age. Late Serravallian (14.2–11.62 Ma).

Characteristics. This zone comprises the FADs of *Crassoretitriletes vanraadshooveni*, *Paleosantalaceaepites cingulatus*, *Psilastephanoporites tesseroporus*, and *Retipollenites crotonicolumellatus* and the last records of *Bombacacidites araracuarensis*, *Bombacacidites nacimientoensis*, *Corsinipollenites oculusnoctis*, *Crototricolpites* cf. *annemariae*, *Ladakhipollenites simplex*, *Mauritiidites crassibaculatus*, and *Cyathidites congoensis*. Also occurring in this zone are *Ctenolophinidites suigeneris*, *Deltoidospora adriennis*, *Echitriporites cricotriporatiformis*, *Laevigatosporites* spp., *Laevigatosporites catanejensis*, *Magnastriatites grandiosus*, *Mauritiidites franciscoi* var. *franciscoi*, *Polypodiisporites* spp., *Polypodiisporites usmensis*, *Psilamonocolpites* spp., and *Retitricolpites simplex*. *Leiosphaeridia* sp., prasinophyceans (algae), and indeterminate dinoflagellate cysts occur frequently (see Appendices 1–6 for details and Figures 2–6 for summary and correlations).

Comparison. The characteristic co-occurrence of taxa (see Tables 5–6 and Figures 2–4 for details) supports the correlation of this zone with other zones in South America (summarized in Figure 5; Lorente 1986; Muller et al. 1987; Hoorn 1993; Jaramillo et al. 2011). This zone is coeval with the T-15 *Crassoretitriletes vanraadshooveni* Zone and the lower part of the T-16 Zone from Llanos in Colombia (Jaramillo et al. 2011), where the LAD of *Mauritiidites crassibaculatus* (as in the Maynas-1 well) occurs. The upper boundary of our zone occurs in La Frontera-1 before the first record of *Ladakhipollenites caribbiensis* that is known from the Late Miocene (da Silva et al. 2010). The lower limit of the Mar-D Zone in the Nahuapa-24X well coincides with that of the T-15 Zone (Figure 6) of Jaramillo et al. (2011). Our zone comprises the FAD of *Retipollenites crotonicolumellatus*, which also occurs in the T-15 Zone, the FADs of both *Paleosantalaceaepites cingulatus* and *Psilastephanoporites tesseroporus*, and the LAD of *Mauritiidites crassibaculatus*, which also occurs in the T-16 Zone of Jaramillo et al. (2011). Therefore, these presences also emphasize the age given to our zone and their correlation (Figures 2–6).

6.5. Mar-E Psilastephanoporites tesseroporus *Interval Zone*

Reference section. La Frontera-1 interval 2220–1540 (677–469 m).

Distribution. This zone was present only in the La Frontera-1 well, interval 2220–1540 ft (677–469 m). Note that in the other wells, samples were not analyzed above the top of the Mar-D zone (see Appendices 1–6 for details and Figures 2–6 for summary and correlations). Nevertheless, GraphCor confirmed this zone as defined here.

Description. We propose the Mar-E *Psilastephanoporites tesseroporus* Interval Zone as occurring from the LAD of *Corsinipollenites oculusnoctis* and/or that of *Cyathidites congoensis* (top of the lower zone) to the LAD of *Psilastephanoporites tesseroporus* and/or the LAD of *Siltaria santaisabelensis*.

Age. Early Tortonian to Late Messinian (11.62–5.48 Ma).

Characteristics. This zone includes the inception and presence of pollen grains of *Ctenolophonidites suigeneris*, *Foveotricolporites lenticuloides*, *Lanagiopollis crassa*, *Paleosantalaceaepites cingu*latus, *Nijssenosporites fossulatus*, and *Retimonocolpites maximus* and the LADs of *Acaciapollenites myriosporites*, *Deltoidospora adriennis*, *Ladakhipollenites caribbiensis*, *Psilastephanoporites tesseroporus*, and *Siltaria santaisabelensis*. Other taxa such as *Osmundacidites ciliatus* and dinoflagellate cysts *Bosedinia infragranulata*, *Quadrina*? *condita* and *Selenopemphix quanta* along with *Echiperiporites estelae*, *Magnastriatites grandiosus*, and *Rhoipites hispidus* are common.

Comparison. This zone is coeval with the *Echitricolporites spinosus* Zone from northern South America (Muller et al. 1987) and can be compared with the upper part of the T-16 *Fenestrites spinosus* Zone of Jaramillo et al. (2011), where the LAD of *Ladakhipollenites*? *caribbiensis* occurs, and to the lower part of the T-17 *Cyatheacidites annulatus* Zone of Jaramillo et al. (2011), where the LAD of *Psilastephanoporites tesseroporus* occurs (upper boundary of our Mar-E zone) (Figures 2–6).

6.6. *Mar-F* Ctenolophonidites suigeneris *Zone*

Reference section. La Frontera-1 interval 1560–1180 ft (475–360 m).

Distribution. This local zone was only identified in the La Frontera-1 well, interval 1540–1180 ft (469–360 m). Note that in the other wells, samples were not analyzed above the top of the Mar-D zone (see Appendices 1–6 for details and Figures 2–6 for summary and correlations).

Description. We propose the Mar-F *Ctenolophonidites suigeneris* Zone for the interval from the LAD of *Psilastephanoporites tesseroporus* (5.48 Ma) to the LADs of *Ctenolophonidites suigeneris* (3.6 Ma) and/or *Cistacearumpollenites rotundiporus* (LAD Pliocene). Note that samples above 1180 ft (360 m) were not analyzed.

Age. Latest Messinian to Zanclean (5.48–3.6 Ma).

Characteristics. This zone comprises the inception or frequent presence of *Deltoidospora* spp., *Echiperiporites akanthos*, *Echiperiporites estelae*, *Laevigatosporites ovatus*, *Lanagiopollis* cf. *crassa*, *Magnastriatites grandiosus*, *Mauritiidites franciscoi* var. *minutus*, *Monoporopollenites annulatus*, *Polypodiisporites usmensis*, *Retimonocolpites maximus*, and *Retitriletes* sp. *Fusiformisporites* is common among the fungal spores. The last records of *Siltaria hammenii* (Neogene), *Cistacearumpollenites rotundiporus* (LAD Pliocene), and *Crassoretitriletes vanraadshooveni* (3.4 Ma) occur in this zone. Noticeable is the absence of *Echitricolporites mcneillyi.*

Comparison. This zone is coeval with the *Psilatricolporites caribbiensis* Subzone from Venezuela (Lorente 1986), due to the absence of *Echitricolporites mcneillyi*, and can be compared with the lower part of the *Echitricolporites mcneillyi* Zone of northern South America (Muller et al. 1987), where the LAD of *Psilastephanoporites tesseroporus* occurs (upper boundary of our Mar-E zone). The upper part of T-17 and the lower part of T-18 (Jaramillo et al. 2011) are also correlated (Figures 2–6).

7. Correlation with other Western Amazonian basins and discussion

The vertical succession of species in the six wells investigated from the Marañon Basin (see Appendices 1–6 for details) allowed us to propose the first palynozonation in a chronostratigraphic context (Figure 5). The presence of selected species in some or all of the boreholes and their stratigraphic ranges (FAD and LAD ages; Figures 2–3 and Tables 5–6) were used to date our zones and establish correlations with relatively coeval palynozones in South America (Figure 6). Some diachronisms exist between the ages of published palynozones from northern South America and ours. For instance, the Early Miocene to earliest Middle Miocene in Venezuela was characterized by the successive *Verrutricolporites* and *Psiladiporites–Echitricolporites* pollen zones (Lorente 1986). These zones are equivalent to the *Verrutricolporites rotundiporus–Echidiporites barbeitoensis* and *Echitricolporites maristellae–Psiladiporites minimus* zones defined by Muller et al. (1987). The *Verrutricolporites* Interval Zone and the *Verrutricolporites rotundiporus–Echidiporites barbeitoensis* Zone are defined as extending from the first records of *Verrutricolporites rotundiporus* to the first occurrence of *Psiladiporites minimus* or *Echitricolporites maristellae*.

Hence, the *Verrutricolporites* (Lorente 1986) and the *Verrutricolporites rotundiporus–Echidiporites barbeitoensis* (Muller et al. 1987) zones can be correlated with our Mar-A *Corsinipollenites oculusnoctis* Interval Zone. In addition, the *Psiladiporites–Echitricolporites* Interval Zone (Lorente 1986) and the *Echitricolporites maristellae–Psiladiporites minimus* Zone (Muller et al. 1987) are defined by the first occurrence of *Psiladiporites minimus* or *Echitricolporites maristellae* at the base, and the first occurrence of *Crassoretitriletes vanraadshooveni* at the top. These markers also correlate with our Mar-B *Malvacipolloides* (*Echitricolporites*) *maristellae* and Mar-C *Mauritiidites crassibaculatus* zones. Hence, our Mar-A, Mar-B, and Mar-C zones are within the Early Miocene to earliest Middle Miocene pollen zones of Lorente (1986) and Muller et al. (1987). Our Mar-A, Mar-B, and Mar-C zones are also coeval with the T-12 *Horniella lunarensis*, T-13 *Echitricolporites maristellae*, and T-14 *Grimsdalea magnaclavata* zones, respectively, of Jaramillo et al. (2011).

The late Early Miocene in Venezuela and in Western Amazonia was characterized by Lorente (1986) and Hoorn (1993), respectively, by the *Crassoretitriletes* Interval Zone. This zone is defined from the first records of *Crassoretitriletes vanraadshooveni* and *Trichotomocolpites* sp. to the first occurrence of *Grimsdalea magnaclavata* in the latest Middle Miocene (Lorente 1986; Hoorn 1993). The top of this zone was defined by Muller et al. (1987) based on the first record of *Echitricolporites spinosus* in the earliest Tortonian. The FAD of *Grimsdalea magnaclavata sensu* Jaramillo et al. (2011) is the oldest at ca. 16.1 Ma, meaning that this FAD would occur before that of *Crassoretitriletes vanraadshooveni.*

We have identified in Arabela-1X, Tigrillo-30X, Nahuapa-24X, and La Frontera-1 wells an interval similar to the *Crassoretitriletes* Interval Zone, by the presence of three biostratigraphic markers, *Crassoretitriletes vanraadshooveni*, *Psilastephanoporites tesseroporus*, and *Retipollenites crotonicolumellatus* (Tables 5–6) co-occurring at the base, which belong to the bases of both the T-15 *Crassoretitriletes vanraadshooveni* palynozone (Jaramillo et al. 2011) and the *Crassoretitriletes* palynozone (Lorente 1986). GraphCor indicated the FAD of *Retipollenites crotonicolumellatus* was slightly below the FADs of *Crassoretitriletes vanraadshooveni* and *Psilastephanoporites tesseroporus.* However, this might be explained by the quality of sampling. The top is identified by *Corsinipollenites oculusnoctis*, *Cyathidites congoensis* and *Mauritiidites crassibaculatus* at ca. 11.62 Ma (Serravallian/Tortonian limit), as shown in the *Crassoretitriletes vanraadshooveni* Interval Zone of Muller et al. (1987). Therefore, the base of our Mar-D *Crassoretitriletes vanraadshooveni* Zone is coeval with the bases of the *Crassoretitriletes vanraadshooveni* zones of Hoorn (1993), Lorente (1986), and Jaramillo et al. (2011), whereas the top is coeval with the top of the *Crassoretitriletes vanraadshooveni* Interval Zone *sensu* Muller et al. (1987). Our Mar-D *Crassoretitriletes vanraadshooveni* Zone is also coeval with the *Crassoretitriletes* Interval Zone of Lorente (1986), recognized by Leite et al. (2017) in the Solimões Basin (Brazil).

The late Miocene from northern South America is characterized by the *Echitricolporites spinosus* Zone (Muller et al. 1987), so our Mar-E zone is coeval and can be also compared with the upper part of the T-16 *Fenestrites spinosus* Zone of Jaramillo et al. (2011), where the LAD of *Ladakhipollenites*? *caribbiensis* occurs. It is also correlated to the lower part of the T-17 *Cyatheacidites annulatus* Zone of Jaramillo et al. (2011), in which the LAD of *Psilastephanoporites tesseroporus* occurs (upper boundary of our Mar-E zone: 5.48 Ma). Although sediments referable to Mar-E and Mar-F zones were studied only in the Fontera-1 well, GraphCor displays the events limiting these zones. Furthermore, due to the abovementioned correlations this interval has a preliminary zonal character which can be improved with additional biostratigraphic studies above the upper section of the studied wells.

Some authors have suggested that there is no record of Pliocene deposits in the Solimões Basin (Latrubesse et al. 2007, 2010). However, recent palynostratigraphic studies (da Silva et al. 2010; Silveira and Souza 2015, 2016; Leite et al. 2017) have documented Pliocene sedimentation in some areas of the Solimões Basin. These palynological studies are based on the presence of the *Psilatricolporites caribbiensis* Interval Subzone (Late Miocene to Early Pliocene: 5.6–3.7 Ma; Lorente 1986) and the *Alnipollenites verus* Interval Subzone (Late Pliocene to Holocene: 3.7 to present; Lorente 1986) found in the studied Solimões wells. Similarly, our study showed that Neogene sedimentation in the Marañon Basin continued during the Pliocene, where at least 360 ft (103 m) of the Marañon formation sediments were deposited (see La Frontera-1 well, Appendix 6 and Figures 4–6). We propose that the Mar-F *Ctenolophonidites suigeneris* Zone (Late Miocene to Early Pliocene, 5.48–3.6 Ma) comprises the youngest deposits dated here. However, since we did not analyze sediments above 1180 ft (356 m), we cannot exclude the possibility of the younger sediments belonging to the *Alnipollenites verus* Interval Subzone *sensu* Lorente (1986) or any coeval zone at depths over 1180 ft (356 m), and/or any coeval zone at depths over those of the last intervals from the other wells studied herein for the Marañon Basin.

8. Conclusions

This study of the Neogene biostratigraphic record obtained from six industrial wells in the Marañon Basin allowed us to define six palynozones (Mar-A to Mar-F); five of them (Mar-A to Mar-E) were validated by GraphCor. They range from the Aquitanian (Early Miocene) to the Messinian–Zanclean (latest Miocene to earliest Pliocene):

- The Mar-A *Corsinipollenites oculusnoctis* Interval Zone (Aquitanian to early Burdigalian: 23.03–17.71 Ma) is defined as extending from the first occurrence of *Retitricolporites wijmstrae*, occurring immediately over the *Cicatricosisporites dorogensis* marker species (latest Oligocene), to the first appearance of *Malvacipolloides maristellae*.
- The Mar-B *Malvacipolloides maristellae* Interval Zone (Burdigalian: 17.71–16.1 Ma) is recognized from the first appearance of *Malvacipolloides maristellae* to the last record of *Retitricolporites wijmstrae*.
- The Mar-C *Mauritiidites crassibaculatus* Assemblage Zone (latest Burdigalian to Late Langhian: 16.1–14.2/13.9 Ma) is defined as occurring from the last record of *Retitricolporites wijmstrae* (top of the lower zone) or the first appearance of *Grimsdalea magnaclavata* (e.g. the Nahuapa-24X well) to the first occurrence of *Crassoretitriletes vanraadshooveni* or *Psilastephanoporites tesseroporus*.
- The Mar-D *Crassoretitriletes vanraadshooveni* Assemblage Zone (Late Serravallian: 14.2–11.62 Ma) is defined by the first occurrence of *Crassoretitriletes vanraadshooveni* and or that of *Psilastephanoporites tesseroporus* at its base and by the last record of *Cyathidites congoensis* and *Mauritiidites crassibaculatus* or *Corsinipollenites oculusnoctis* at its top (e.g. La Frontera-1 well).
- The Mar-E *Psilastephanoporites tesseroporus* local Interval Zone (Early Tortonian to Late Messinian: 11.62–5.48 Ma) represents the time interval with *Psilastephanoporites tesseroporus* from the last occurrence of *Corsinipollenites oculusnoctis* and/or *Cyathidites congoensis* to the last occurrence of *Psilastephanoporites tesseroporus*. It is dominated by *Psilastephanoporites tesseroporus* and *Siltaria santaisabelensis*.
- The Mar-F *Ctenolophonidites suigeneris* local Zone (latest Messinian to Zanclean: 5.48–3.6 Ma) is defined at its base by the last appearance of *Psilastephanoporites tesseroporus* and at its top by the last occurrence of *Ctenolophonidites suigeneris*. *Cistacearumpollenites rotundiporus* and *Siltaria hammenii* dominate this zone.

The biostratigraphic scheme proposed for the Marañon Basin is based on the presence of species in common with Miocene palynozones of northern South America (Colombia, Venezuela, and western Brazil), and a correlation between them is also established. Our study corroborates recent studies regarding the palynostratigraphy of the Miocene Solimões and Acre basins, and documents that Pliocene sedimentation occurred in Peru (western Amazonia). Future study of the interval above the analyzed wells may provide information to characterize the Pliocene palynofloras of the Marañon Basin. A comparison with Amazonia and elsewhere in northern South American basins will achieve new insights for the less well-known evolution of floras during the Pliocene.

Acknowledgements

This work was supported by the French Research Institute for Development (IRD) under Grant BTDR and by PALEOSEDES E.U. (Colombia) under Grant STU04-2016, as well as by collaboration and partnership with the Toulouse III Paul Sabatier University (France), National University (Colombia), and CICYTTP-CONICET (Argentina) under CONICET PIP 0812. The first author is a PhD candidate and IRD scholarship holder and received Graphic Correlation software training from Dr Jaramillo at STRI, Panama. We thank Perupetro for allowing us to study the ditch-cutting samples and their permission to publish this article. Special thanks are given to Dr C. Jaramillo and another, anonymous reviewer, for their suggestions that allowed us to substantially improve the manuscript.

Disclosure statement

In accordance with Taylor & Francis policy and our ethical obligation as researchers, all the authors state that there is no conflict of interest.

Data availability statement

The data that support the findings of this study are openly available in NeotomaDB at:

Maynas-1 https://apps.neotomadb.org/Explorer/?datasetid=40652
Tucunare-1X https://apps.neotomadb.org/Explorer/?datasetid=40785
Arabela-1X https://apps.neotomadb.org/Explorer/?datasetid=40947
Frontera-1 https://apps.neotomadb.org/Explorer/?datasetid=40956
Nahuapa-24X https://apps.neotomadb.org/explorer/?datasetid=40965
Tigrillo-30X https://apps.neotomadb.org/explorer/?datasetid=40995

Notes on contributors

Francisco Parra has obtained a MSc Degree in Geology of Natural Resources at the University of Toulouse, France. He is currently a PhD student in co-tutorship at the University of Toulouse and the National University of Colombia, funded by the IRD. His experience mainly spans sedimentology and stratigraphy combining laboratory and field work with a focus in post-Paleozoic micropaleontology (foraminifers, ostracods, spores, pollen, dinoflagellates, and charophytes), biostratigraphy, paleogeography, paleoenvironmental analysis in Colombian and Peruvian Amazonia.

Rosa E. Navarrete is a PhD geologist, micropaleontologist and biostratigrapher, mainly focused on marine and terrestrial environments, tectonic – erosion, paleogeography and paleoclimate. She is much experienced in multidisciplinary biogeochronology (foraminifers, ostracods, calcareous nannofossils, mollusks, and palynostratigraphy) of the post-Paleozoic interval in Americas, with emphasis on South American sedimentary basins. She is Chairwoman and research senior of biostratigraphy consulting Colombian company Paleosedes E.U. assessing Oil & Gas industry over 25 years.

Mercredes di Pasquo Ph.D. 1999. Univ. Buenos Aires, Argentina. 2002: CONICET permanent researcher. 2010: Senior researcher, responsible Paly-Lab, CICYTTP. 2009-2020: President ALPP. 2009: Fulbright Research Fellow - Univ. Idaho. 2013-14: Researcher of "Ciencias sem Fronteiras" -CNPq in Brazil. Researches on palynofloras of Silurian/ Permian Arg/ Bolivia/Peru/Brazil, Dev-Carb Montana, Cret. Antarctica, Holoc. Entre Rıos. Supervisor PhD students from America. Phanerozoic Oil industry consultant.

Martin Roddaz is an Associate Professor of geology in the University of Toulouse, France. His main scientific interests include the understanding on controls on sediment production, transport and deposition in the Andes-Amazon system at both short and geological timescales. He has participated in or led several field expeditions in the Amazon basin (Peru, Bolivia) since 2001. He is WP2 Leader of CLIMAMAZON project (Joint Brazilian–European facility for climate and geodynamic research on the Amazon River Basin sediments, http://www.clim-amazon.eu/).

Ysabel Calderón is a geologist working at PERUPETRO, Private Law State Company of the Energy and Mines Peruvian Sector. Since joining PERUPETRO in 2000, she evaluated new plays and promoted areas in different basins of Peru (Offshore and Onshore basins). Also, she is a PhD student at Géosciences-Environnement Toulouse in Paul Sabatier University, France, funded by the Institut de Recherche pour le Développement. She obtained a Master degree in Geology from the same university. Her research has been focused on structural architecture, sedimentary evolution and hydrocarbon potential in a wedge-top foredeep zone in the northern Peruvian subandean basins.

Patrice Baby is a geologist. He is Research Director at the Institute for Research and Development. He has a PhD in Earth sciences from the University of Toulouse, France. His works focus mainly on Andean, Subandean, and Amazonian geodynamics. In the last 20 years, he has cooperated with academic and industrial institutions in Bolivia, Peru, and Ecuador. In the last decade, he has also beenworkingwith biologists and paleontologists on the tectonic control of the diversification of biota in Western Amazonia. In particular, he has launched the multidisciplinary research group primarily coinciding with the coauthors of this review, and led several geological-paleontological expeditions in Amazonia.

ORCID

F.J. Parra http://orcid.org/0000-0003-0801-9446
R.E. Navarrete http://orcid.org/0000-0003-0131-352X
M.M. di Pasquo http://orcid.org/0000-0003-3068-0089
M. Roddaz http://orcid.org/0000-0001-8562-8582
Y. Calderón http://orcid.org/0000-0003-1060-4425
P. Baby http://orcid.org/0000-0001-6142-5174

References

Antoine P-O, Abello MA, Adnet S, Altamirano Sierra AJ, Baby P, Billet G, Boivin M, Calderón Y, Candela A, Chabain J. 2016. A 60-Million-year Cenozoic history of western Amazonian ecosystems in Contamana, eastern Peru. Gondwana Research. 31:30–59.

Baby P, Calderón Y, Louterbach M, Espurt N, Brusset S, Roddaz M, Brichau S, Eude A, Calves G, Quispe A, Ramirez L, Bandach A, Bolanos R. 2018. The peruvian sub-Andean Foreland Basin System: Structural overview, geochronologic constraints, and unexplored plays. In: Zamora G, McClay KR, Ramos VA, editors. Petroleum Basins and Hydrocarbon Potential of the Andes of Peru and Bolivia, v. Memoir 117, AAPG, p. 91–120.

Boonstra M, Ramos MI, Lammertsma EI, Antoine P-O, Hoorn C. 2015. Marine connections of Amazonia: evidence from foraminifera and dinoflagellate cysts (early to middle Miocene, Colombia/Peru). Palaeogeography, Palaeoclimatology, Palaeoecology. 417:176–194.

Bujak JP, Williams GL. 1985. Mesozoic and Cenozoic dinoflagellates. Plankton stratigraphy. Cambridge: Cambridge University Press; p. 847–965.

Calderón Y, Baby P, Hurtado C, Brusset S. 2017a. Thrust tectonics in the Andean retro-foreland basin of northern Peru: Permian inheritances and petroleum implications. Marine and Petroleum Geology. 82: 238–250. doi:10.1016/j.marpetgeo.2017.02.009

Calderón Y, Vela Y, Hurtado C, Bolaños R, Baby P, Eude A, Roddaz M, Brusset S, Calvès G. 2017b. Petroleum systems restoration of the Huallaga—Marañon Andean retroforeland basin, Peru. In: AbuAli MA, Moretti I, Nordgård Bolås HM, editors. Petroleum systems analysis—case studies. AAPG; p. 95–116. Elsevier. doi:10.1016/j.marpetgeo.2017.02.009

Cole JM. 1992. Freshwater dinoflagellate cysts and acritarchs from Neogene and Oligocene sediments of the South China Sea and adjacent areas, in: Head, M.J., Wrenn, J.H. (Eds.), Neogene and Quaternary dinoflagellate cysts and Acritarchs. American Association of Stratigraphic Palynologists Foundation, Dallas, Texas, pp. 181–196.

da Silva-Caminha SAF, Jaramillo CA, Absy ML. 2010. Neogene palynology of the Solimões basin, Brazilian Amazonia. Palaeontographica Abteilung B. 284(1–3):13–79.

de Verteuil L, Norris G, Head MJ, Wrenn JH. 1992. Miocene protoperidiniacean dinoflagellate cysts from the Maryland and Virginia coastal plain. In: Head MJ, Wrenn JH, editors. Neogene and Quaternary dinoflagellate cysts and acritarchs. Dallas: American Association of Stratigraphic Palynologists Foundation; p. 391–430.

Eisawi A, Schrank E. 2008. Upper Cretaceous to Neogene Palynology of the Melut Basin, Southeast Sudan. Palynology. 32(1):101–129.

Eude A, Roddaz M, Brichau S, Brusset S, Calderón Y, Baby P, Soula JC. 2015. Controls on timing of exhumation and deformation in the northern Peruvian eastern Andean wedge as inferred from low-temperature thermochronology and balanced cross section. Tectonics. 34(4):715–730.

Germeraad JH, Hopping CA, Muller J. 1968. Palynology of Tertiary sediments from tropical areas. Review of Palaeobotany and Palynology. 6(3–4):189–348.

Gingras MK, Rasanen ME, Pemberton SG, Romero LP. 2002a. Ichnology and sedimentology reveal depositional characteristics of bay-margin parasequences in the Miocene Amazonian foreland basin. Journal of Sedimentary Research. 72(6):871–883.

Gingras MK, Räsänen ME, Ranzi A. 2002b. The significance of bioturbated inclined heterolithic stratification in the southern part of the Miocene Solimões Formation, Rio Acre, Amazonia Brazil. Palaios. 17(6):591–601.

González-Guzmán, AE. 1968. A palynological study on the upper los cuervos and mirador formations (Lower and Middle Eocene; Tibú area, Colombia), ed. E. J. Brill. Leiden: Hugo de Vries Laboratory. 68.

Grimm EC. 2005. TILIA and TILIAGRAPH software. Springfield (IL): Illinois State Museum. https://www.tiliait.com/download/

Gross M, Piller WE, Ramos MI, Douglas da Silva Paz J. 2011. Late Miocene sedimentary environments in south-western Amazonia (Solimões Formation, Brazil). Journal of South American Earth Sciences. 32(2):169–181.

Hermoza W. 2004. *Dynamique tectono-sedimentaire et restauration sequentielle du retro-bassin d'avant-pays des Andes Centrals* [Unpublished Ph.D. thesis]. Toulouse: Université Paul Sabatier; p. 296.

Hermoza W, Baby P, Brusset S, Roddaz M, Bolaños R. 2005. Eocene to present-day latitudinal variations in the retroforeland basin system of the Peruvian Andes.: 6th International Symposium on Andean Geodynamics (ISAG 2005). Extended Abstracts, p. 368–371

Hermoza W, Brusset S, Baby P, Gil W, Roddaz M, Guerrero N, Bolaños R. 2005. The Huallaga foreland basin evolution: thrust propagation in deltaic environment, in the northern Peruvian Andes. Journal of South American Earth Sciences. 19(1):21–34.

Hood KC. 1998. GraphCor Interactive Graphic Correlation Software. Version 3.0. Houston.

Hoorn C. 1993. Marine incursions and the influence of Andean tectonics on the Miocene depositional history of northwestern Amazonia: results of a palynostratigraphic study. Palaeogeography, Palaeoclimatology, Palaeoecology. 105(3–4):267–309.

Hoorn C. 1994a. An environmental reconstruction of the palaeo-Amazon river system (middle–late Miocene Amazonia). Palaeogeography, Palaeoclimatology, Palaeoecology. 112(3–4):187–238.

Hoorn C. 1994b. Fluvial palaeoenvironments in the intracratonic Amazonas basin (early Miocene-early middle Miocene, Colombia). Palaeogeography, Palaeoclimatology, Palaeoecology. 109(1):1–54.

Hoorn C. 2006. Mangrove forests and marine incursions in Neogene Amazonia (lower Apaporis river, Colombia). Palaios. 21(2):197–209.

Hoorn C, Bogotá-A GR, Romero-Baez M, Lammertsma EI, Flantua SGA, Dantas EL, Dino R, do Carmo DA, Chemale FJ. 2017. The Amazon at sea: Onset and stages of the Amazon river from a marine record, with special reference to Neogene plant turnover in the drainage basin. Global and Planetary Change. 153:51–65.

Hoorn C, Guerrero J, Sarmiento GA, Lorente MA. 1995. Andean tectonics as a cause for changing drainage patterns in Miocene northern South America. Geology. 23(3):237.

Hoorn C, Paxton CGM, Crampton WGR, Burgess P, Marshall LG, Lundberg JG, Räsänen ME, Linna AM. 1996. Miocene deposits in the Amazonian foreland basin. Science. 273(5271):122–120.

Hoorn C, Wesselingh FP. 2010. Amazonia, landscape and species evolution: a look into the past. Chichister: Wiley-Blackwell Publishing Ltd.

Hoorn C, Wesselingh FP, Hovikoski J, Guerrero J. 2010a. The development of the Amazonian mega-wetland (Miocene; Brazil, Colombia, Peru, Bolivia). In: Amazonia, landscape and species evolution: a look into the past. Chichester: Wiley-Blackwell Publishing Ltd; p. 123–142.

Hoorn C, Wesselingh FP, ter Steege H, Bermudez MA, Mora A, Sevink J, Sanmartin I, Sanchez-Meseguer A, Anderson CL, Figueiredo JP, et al. 2010b. Amazonia through time: Andean uplift, climate change, landscape evolution, and biodiversity. Science. 330(6006):927–931.

Hovikoski J, Gingras M, Rasanen M, Rebata LA, Guerrero J, Ranzi A, Melo J, Romero L, del Prado HN, Jaimes F. 2007. The nature of Miocene Amazonian epicontinental embayment: high-frequency shifts of the low-gradient coastline. Geological Society of America Bulletin. 119(11–12):1506–1520.

Hovikoski J, Räsänen M, Gingras M, Lopéz S, Romero L, Ranzi A, Melo J. 2007. Palaeogeographical implications of the Miocene Quendeque Formation (Bolivia) and tidally-influenced strata in southwestern Amazonia. Palaeogeography, Palaeoclimatology, Palaeoecology. 243(1–2):23–41.

Hurtado C, Roddaz M, Santos RV, Baby P, Antoine P-O, Dantas EL. 2018. Cretaceous-early Paleocene drainage shift of Amazonian rivers driven by equatorial Atlantic ocean opening and Andean uplift as deduced from the provenance of northern Peruvian sedimentary rocks (Huallaga basin). Gondwana Research. 63:152–168.

Jaramillo CA, Rueda M. 2019. A morphological electronic database of Cretaceous-Tertiary and extant pollen and spores from northern South America. http://biogeodb.stri.si.edu/jaramillosdb/web/morphological/.

Jaramillo CA, Hoorn C, da Silva SAF, Leite F, Herrera F, Quiroz L, Dino R, Antonioli L. 2010. The origin of the modern Amazon rainforest: implications of the palynological and palaeobotanical record. In: Hoorn C, Wesselingh FP, editors. Amazonia, landscape and species evolution: a look into the past. Chichister: Wiley-Blackwell Publishing Ltd; p. 317–334.

Jaramillo C, Romero I, D'Apolito C, Bayona G, Duarte E, Louwye S, Escobar J, Luque J, Carrillo-Briceño JD, Zapata V, et al. 2017. Miocene flooding events of western Amazonia. Science Advances. 3(5):e1601693.

Jaramillo CA, Rueda M, Torres V. 2011. A palynological zonation for the Cenozoic of the Llanos and Llanos foothills of Colombia. Palynology. 35(1):46–84.

Latrubesse EM, Cozzuol M, da Silva SAF, Rigsby CA, Absy ML, Jaramillo CA. 2010. The late Miocene paleogeography of the Amazon basin and the evolution of the Amazon river system. Earth-Science Reviews. 99(3–4):99–124.

Latrubesse EM, da Silva SAF, Cozzuol M, Absy ML. 2007. Late Miocene continental sedimentation in southwestern Amazonia and its regional significance: biotic and geological evidence. Journal of South American Earth Sciences. 23(1):61–80.

Leandro LM, Vieira CEL, Santos A, Fauth G. 2019. Palynostratigraphy of two Neogene boreholes from the northwestern portion of the Solimões basin, Brazil. Journal of South American Earth Sciences. 89:211–218.

Leite FPR, Paz J, do Carmo DA, Silva-Caminha SA. 2017. The effects of the inception of Amazonian transcontinental drainage during the Neogene on the landscape and vegetation of the Solimões basin, Brazil. Palynology. 41(3):412–422.

Linhares AP, Ramos Feijó MI. 2011. Evidence for marine influx during the Miocene in southwestern Amazonia, Brazil. Geología Colombiana. 36(1):91–103

Linhares AP, Ramos MIF, Gaia VCS, Friaes YS. 2019. Integrated biozonation based on palynology and ostracods from the Neogene of Solimões Basin, Brazil. Journal of South American Earth Sciences. 91: 57. doi:10.1016/j.jsames.2019.01.015.

Linhares AP, de Souza Gaia VC, Ramos MI. 2017. The significance of marine microfossils for paleoenvironmental reconstruction of the Solimões Formation (Miocene), western Amazonia, Brazil. Journal of South American Earth Sciences. 79:57–66.

Lorente MA. 1986. Palynology and palynofacies of the Upper Tertiary in Venezuela. Berlin and Stuttgart: Lubrecht & Cramer Ltd

Louterbach M, Roddaz M, Antoine P-O, Marivaux L, Adnet S, Bailleul J, Dantas E, Santos RV, Chemale F, Baby P, et al. 2018. Provenance record of late Maastrichtian–late Paleocene Andean mountain building in the Amazonian retroarc foreland basin (Madre de Dios basin, Peru). Terra Nova. 30(1):17–23.

Macphail MK. 1999. Palynostratigraphy of the Murray basin, inland southeastern Australia. Palynology. 23(1):197–240.

Mann KO, Lane HR. 1995. Graphic correlation: a powerful stratigraphic technique comes of age. SEPM Special Publication 53, Tulsa, p. 262.

Marocco R, Bolanos R, Paz M, Tarazona A. 1995. Informe preliminar sobre el estudio de la sedimentación neógena del nororiente del Perú en base al análisis de los pozos Tangarana 18-4x, Jibaro 1, Valencia 25x, Chapuli 20-1x, Maranon 10-1x, Cuinico norte 6-46x, Nahuaca 3x, Tapiche 36-2x, la Frontera 46-3x. [preliminary report about the study of Neogene sedimentation, northeast Peru on the basis of the analysis of wells Tangarana 18-4x, Jibaro 1, Valencia 25x, Chapuli 20-1x, Maranon 10-1x, Cuinico norte 6-46x, Nahuaca 3x, Tapiche 36-2x, la Frontera 46-3x]. Lima: ORSTOM, PETROPERU.

Mathalone JMP, Montoya MR. 1995. Petroleum geology of the sub-Andean basins of Peru. In: Tankard AJ, Suárez-Soruco R, Welsink HJ, editors. Petroleum basins of South America. Houston (MA): AAPG; p. 423–444.

Monsch KA. 1998. Miocene fish faunas from the northwestern Amazonia basin (Colombia, Peru, Brazil) with evidence of marine incursions. Palaeogeography, Palaeoclimatology, Palaeoecology. 143(1–3):31–50.

Muller J, Di Giacomo E, Van Erve AW. 1987. A palynological zonation for the Cretaceous, Tertiary Quaternary of northern South America. Dallas (TX): American Association of Stratigraphic Palynologists. Contribution Series 19; p. 1–77.

Muñoz-Torres FA, Whatley RC, Van Harten D. 2006. Miocene ostracod (crustacea) biostratigraphy of the upper Amazon basin and evolution of the genus *Cyprideis*. Journal of South American Earth Sciences. 21(1–2):75–86.

Raine JI, Mildenhall DC, Kennedy EM. 2011. New Zealand fossil spores and pollen: an illustrated online catalogue. 4th ed. Lower Hutt: GNS Science. http://data.gns.cri.nz/sporepollen/index.htm.

Ramos MI. 2006. Ostracods from the Neogene Solimões Formation (Amazonas, Brazil). Journal of South American Earth Sciences. 21(1–2): 87–95.

Räsänen ME, Linna AM, Santos JCR, Negri FR. 1995. Late Miocene tidal deposits in the Amazonian foreland basin. Science (New York, N.Y.). 269(5222):386–390.

Rebata LA, Gingras MK, Räsänen ME, Barberi M. 2006a. Tidal-channel deposits on a delta plain from the upper Miocene Nauta Formation, Marañon foreland sub-basin, Peru. Sedimentology. 53:971–1013.

Rebata LA, Räsänen ME, Gingras MK, Vieira V, Barberi M, Irion G. 2006b. Sedimentology and ichnology of tide-influenced late Miocene successions in western Amazonia: the gradational transition between the Pebas and Nauta Formations. Journal of South American Earth Sciences. 21(1–2):96–119.

Regali MSP, Uesugui N, Santos AS. 1974a. Palinologia dos sedimentos Meso-Cenozóicos do Brasil (i). [Palynology of Meso-Cenozoic sediments of Brazil (i).]. Boletim Técnico da Petrobras. 17(3):177–191.

Regali MSP, Uesugui N, Santos AS. 1974b. Palinologia dos sedimentos Meso-Cenozóicos do Brasil (ii). [Palynology of Meso-Cenozoic sediments of Brazil (ii).]. Boletim Técnico da Petrobras. 17(4):263–301.

Roddaz M, Baby P, Brusset S, Hermoza W, Darrozes JM. 2005. Forebulge dynamics and environmental control in western Amazonia: the case study of the arch of Iquitos (Peru). Tectonophysics. 399(1–4):87–108.

Roddaz M, Hermoza W, Mora A, Baby P, Parra M, Christophoul F, Brusset S, Espurt N. 2010. Cenozoic sedimentary evolution of the Amazonian foreland basin system. In: Hoorn H, Wesselingh FP, editors. Amazonia, landscape and species evolution: a look into the past. Chichister: Wiley-Blackwell Publishing Ltd; p. 61–88.

Salas-Gismondi R, Antoine P-O, Baby P, Brusset S, Benammi M, Espurt N, De Franceschi D, Pujos F, Tejada-Lara JV, Urbina M. 2007. Middle Miocene crocodiles from the Fitzcarrald arch. Amazonian Peru. Cuadernos Del Museo Geominero. 8:355–360.

Shaw AB. 1964. Time in stratigraphy. New York (NY): McGraw Hill; p. 365.

Silveira R, Souza P. 2015. Palinologia (grãos de pólen de angiospermas) das formações Solimões e Içá (bacia do Solimões), nas regiões de Coari e Alto Solimões, Amazonas. [Palynology (pollen grains of angiosperms) of the Solimões and Içá formations (Solimões basin), in the regions of Coari and Alto Solimões, Amazonas]. Revista Brasileira de Paleontologia. 18(3):455–474.

Silveira R, Souza P. 2016. Palinologia (esporos de fungos e pteridófitas, grãos de pólen de gimnopermas, cistos de algas e escolecodonte) das formações Solimões e Içá (Neogeno e Pleistoceno, bacia do Solimões), Amazonas, Brasil. [Palynology (spores of fungi and ferns, grains gymnosperms pollen, algal cysts and scolecodonts) of the Solimões and Içá formations (Neogene and Pleistocene, the Solimões basin), Amazonas, Brazil.]. Pesquisas em Geociências. 43(1):17–39.

Tryon AF, Lugardon B. 1991. Spores of the pteridophyta: surface, wall structure, and diversity based on electron microscope studies. New York (NY): Springer Science & Business Media.

Van der Hammen T. 1956. Description of some genera and species of fossil pollen and spores. Boletín Geológico. Servicio Geológico Colombiano, Bogota. 4(2–3):111–117.

Wesselingh FP. 2006. Miocene long-lived lake Pebas as a stage of mollusc radiations, with implications for landscape evolution in western Amazonia. Scripta Geologica. 133:1–17.

Wesselingh FP, Guerrero J, Räsänen ME, Romero Pittman L, Vonhof HB. 2006a. Landscape evolution and depositional processes in the Miocene Amazonian Pebas lake/wetland system: evidence from exploratory boreholes in northeastern Peru. Scripta Geologica. 133:323–361.

Wesselingh FP, Hoorn C, Guerrero J, Räsänen ME, Romero Pittman L, Salo JS. 2006b. The stratigraphy and regional structure of Miocene deposits in western Amazonia (Peru, Colombia and Brazil), with implications for late Neogene landscape evolution. Scripta Geologica. 133: 291–322.

Wesselingh FP, Hoorn C, Kroonenberg SB, Antonelli A, Lundberg JG, Vonhof HB, Hooghiemstra H. 2010. On the origin of Amazonian landscapes and biodiversity: a synthesis. In: Hoorn C, Wesselingh FP, editors. Amazonia, landscape and species evolution: a look into the past. Chichister: Wiley-Blackwell Publishing Ltd; p. 419–431.

Wesselingh FP, Ramos MI. 2010. Amazonian aquatic invertebrate faunas (mollusca, ostracoda) and their development over the past 30 million years. In: Hoorn C, Wesselingh FP, editors. Amazonia, landscape and species evolution: a look into the past. Oxford (UK): Wiley-Blackwell Publishing Ltd; p. 302–316.

Whatley RC, Muñoz-Torres FA, Van Harten D. 1998. The ostracoda of an isolated Neogene saline lake in the western Amazon basin. What about Ostracoda. 20:231–245.

Williams GL, Fensome RA, MacRae RA. 2017. Dinoflaj3. American Association of Stratigraphic Palynologists, data series no. 2. http://dinoflaj.smu.ca/dinoflaj3/index.php/Main_Page.

Wood GD, Gabriel AM, Lawson JC. 1996. Palynological techniques – processing and microscopy. In: Jansonius J, McGregor DC, editors. Palynology: Principles and applications. Dallas (TX): American Association of Stratigraphic Palynologists Foundation; Volume 1, p. 29–50.

List of species with author citations

Spores

Cicatricosisporites dorogensis Potonié & Gelletich, 1933
Crassoretitriletes vanraadshooveni Germeraad, Hopping & Müller, 1968
Cyathidites congoensis Sah, 1967
Cyathidites minor Couper, 1953

Deltoidospora adriennis (Potonié & Gelletich, 1933) Frederiksen, 1983
Echinatisporis muelleri (Regali, Uesugui & Santos, 1974) Silva-Caminha, Jaramillo & Absy, 2010
Foveotriletes ornatus Regali, Uesugui & Santos, 1974
Laevigatosporites catanegensis Muller, Di Giacomo & Van Erve, 1987
Laevigatosporites granulatus Jaramillo, Pardo, Rueda, Torres, Harrington, & Mora, 2007
Laevigatosporites ovatus Wilson & Webster, 1946
Magnastriatites grandiosus (Kedves & Sole de Porta, 1963) Dueñas, 1980
Nijssenosporites fossulatus Lorente, 1986
Osmundacidites ciliatus Sah, 1967
Polypodiisporites specious Sah, 1967
Polypodiisporites usmensis (Van der Hammen, 1956) Khan & Martin, 1972
Retitriletes altimuratus Silva-Caminha, Jaramillo & Absy, 2010
Striatriletes saccolomoides Jaramillo, Rueda & Torres, 2011
Verrutriletes virueloides Jaramillo, Pardo, Rueda, Torres, Harrington & Mora, 2007

Pollen grains

Acaciapollenites myriosporites (Cookson, 1954) Mildenhall, 1972
Araliaceoipollenites Jussieu, 1789
Arecipites perfectus Silva-Caminha, Jaramillo & Absy, 2010
Bombacacidites soleaformis Muller, Di Giacomo & Van Erve, 1987
Bombacacidites annae (Van der Hammen, 1954) Leidelmeyer, 1966
Bombacacidites araracuarensis Hoorn, 1994
Bombacacidites brevis (Dueñas, 1980) Muller, Di Giacomo & Van Erve, 1987
Bombacacidites gonzalezi Jaramillo & Dilcher, 2001
Bombacacidites nacimientoensis (Anderson, 1960) Elsik, 1968
Bombacacidites psilatus Jaramillo & Dilcher, 2001
Catostemma type Bentham, 1843
Cistacearumpollenites rotundiporus Silva-Caminha, Jaramillo & Absy, 2010
Clavainaperturites clavatus Van der Hammen & Wymstra, 1964
Colombipollis tropicalis Sarmiento, 1992
Corsinipollenites psilatus Jaramillo & Dilcher, 2001
Corsinipollenites collaris Silva-Caminha, Jaramillo & Absy, 2010
Corsinipollenites oculusnoctis (Thiergart, 1940) Nakoman, 1965
Corsinipollenites psilatus Jaramillo & Dilcher, 2001
Crassiectoapertites columbianus (Dueñas, 1980) emend. Lorente, 1986
Crototricolpites annemariae Leidelmeyer, 1966
Ctenolophonidites suigeneris Silva-Caminha, Jaramillo & Absy, 2010
Cyclusphaera scabrata Jaramillo & Dilcher, 2001
Echiperiporites estelae Germeraad, Hopping & Müller, 1968
Echiperiporites jutaiensis Silva-Caminha, Jaramillo & Absy, 2010
Echiperiporites akanthos Van der Hammen & Wijmstra, 1964
Echiperiporites estelae Germeraad, Hopping & Müller, 1968
Echiperiporites lophatus Silva-Caminha, Jaramillo & Absy, 2010
Echitriporites trianguliformis van Hoeken-Klinkenberg, 1964
Echitriporites cricotriporatiformis Jaramillo, Rueda & Torres, 2011
Foveotricolporites lenticuloides Silva-Caminha, Jaramillo & Absy, 2010
Gomphrenipollis minimus Silva-Caminha, Jaramillo & Absy, 2010
Grimsdalea magnaclavata Germeraad, Hopping & Müller, 1968
Hedyosmum type Swartz, 1788
Ladakhipollenites simplex (González-Guzmán, 1967) Jaramillo & Dilcher, 2001
Ladakhipollenites? caribbiensis (Muller, Di Giacomo & Van Erve, 1987) Silva-Caminha, Jaramillo & Absy, 2010
Lanagiopollis crassa (Van der Hammen & Wymstra, 1964) Frederiksen, 1988
Magnaperiporites spinosus González-Guzmán, 1967
Malvacipolloides (*Echitricolporites*) *maristellae* (Muller, Di Giacomo & Van Erve, 1987) Silva-Caminha, Jaramillo & Absy, 2010
Margocolporites vanwijhei Germeraad, Hopping & Muller 1968
Mauritiidites crassibaculatus Van Hoeken-Klinkenberg, 1964
Mauritiidites franciscoi franciscoi (Van der Hammen, 1956) van Hoeken-Klinkenberg, 1964
Mauritiidites franciscoi minutus Van der Hammen & Garcia, 1966
Monocolpopollenites ovatus Jaramillo & Dilcher, 2001
Monoporopollenites annulatus (Van der Hammer, 1954) Jaramillo & Dilcher, 2001
Multiporopollenites pauciporatus Jaramillo & Dilcher, 2001
Paleosantalaceaepites cingulatus Jaramillo, Rueda & Torres, 2011
Perfotricolpites digitatus González-Guzmán, 1967
Perisyncolporites pokornyi Germeraad, Hooping & Müller, 1968
Polyadopollenites mariae Dueñas, 1980
Proteacidites triangulatus Lorente, 1986
Proxapertites tertiaria Van der Hammen & Garcia, 1966
Proxapertites minutus Dueñas, 1980
Proxapertites operculatus (Van der Hammen, 1954) Van der Hammen, 1956
Proxapertites psilatus Sarmiento, 1992
Proxapertites verrucatus Sarmiento, 1992
Psilamonocolpites medius (Van der Hammen, 1954) Van der Hammen & Garcia, 1966
Psilastephanocolporites fissilis Leidelmeyer, 1966
Psilastephanoporites tesseroporus Regali, Uesugui & Santos, 1974
Psilatricolpites papilioniformis Regali, Uesugui & Santos, 1974
Psilatricolporites garzoni Hoorn, 1993
Psilatricolporites operculatus Van der Hammen & Wijmstra, 1964
Psilatricolporites crassoexinatus Hoorn, 1993
Psilatricolportires operculatus minutus González-Guzmán, 1967
Ranunculacidites operculatus (van der Hammen & Wijmstra, 1964) Jaramillo & Dilcher, 2001
Retibrevitricolporites yavarensis (Hoorn, 1993) Silva-Caminha, Jaramillo & Absy, 2010
Retimonocolpites maximus Hoorn, 1993
Retimonocolpites retifossulatus Lorente, 1986
Retipollenites crotonicolumellatus Jaramillo, Rueda & Torres, 2011
Retistephanocolporites fossulatus Jaramillo & Dilcher, 2001
Retistephanoporites angelicus González-Guzmán, 1967
Retistephanoporites crassiannulatus Lorente, 1986
Retitrescolpites irregularis (Van der Hammen & Wymstra, 1964) Jaramillo & Dilcher, 2001
Retitrescolpites magnus (González-Guzmán, 1967) Jaramillo & Dilcher, 2001
Retitrescolpites saturum (González-Guzmán, 1967) Jaramillo & Dilcher, 2001
Retitricolpites simplex González-Guzmán, 1967
Retitricolpites colpiconstrictus Hoorn, 1994
Retitricolpites simplex González-Guzmán, 1967
Retitricolporites wijmstrae Hoorn, 1994
Retitriporites dubiosus González-Guzmán, 1967
Rhoipites guianensis (Van der Hammen & Wymstra, 1964) Jaramillo & Dilcher, 2001
Rhoipites hispidus (Van der Hammen & Wymstra, 1964) Jaramillo & Dilcher, 2001
Siltaria hammenii Silva-Caminha, Jaramillo & Absy, 2010
Siltaria santaisabelensis (Hoorn, 1994) Silva-Caminha, Jaramillo & Absy, 2010
Spirosyncolpites spiralis González-Guzmán, 1967
Tetracolporopollenites maculosus (Regali, Uesugui & Santos, 1974) Jaramillo & Dilcher, 2001

Microplankton

Chomotriletes minor Pocock, 1970
Apteodinium australiense Williams, 1978
Selenopemphix quanta (Bradford, 1975) Matsuoka, 1985
Bosedinia infragranulata He, 1984
Operculodinium group Wall, 1967
Polysphaeridium group Davey & Williams, 1966b
Selenopemphix nephroides Benedek, 1972
Retitrescolpites? irregularis (Van der Hammen & Wymstra, 1964) Jaramillo & Dilcher, 2001
Quadrina? condita de Verteuil & Norris, 1992

Appendix 1. Arabela

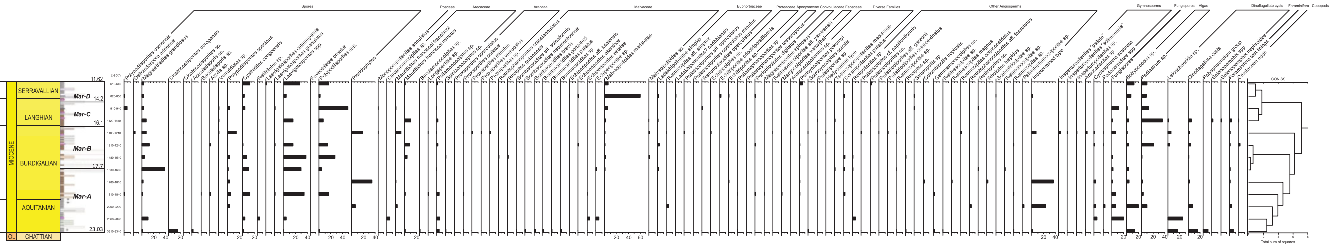

Appendix 2. Maynas

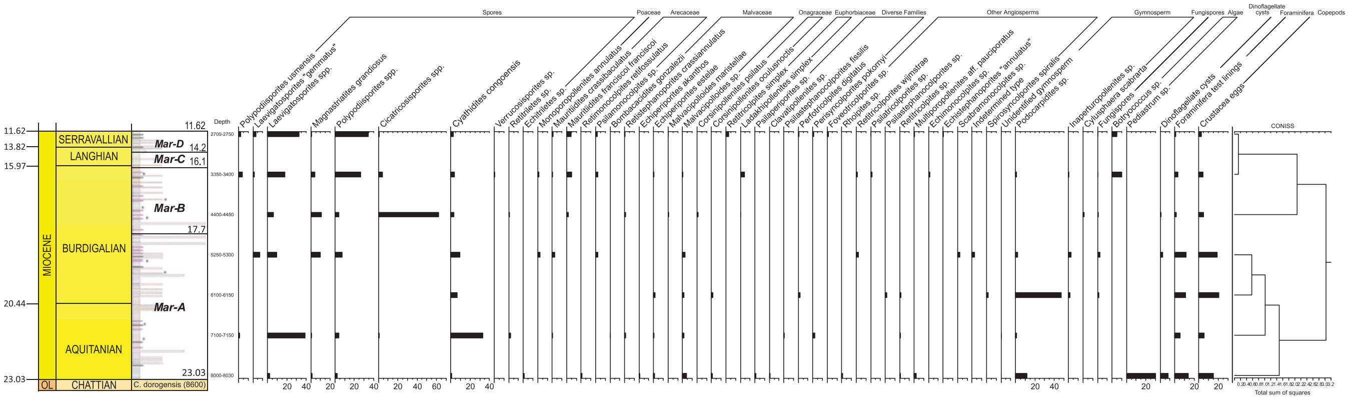

Appendix 3. Tacunare

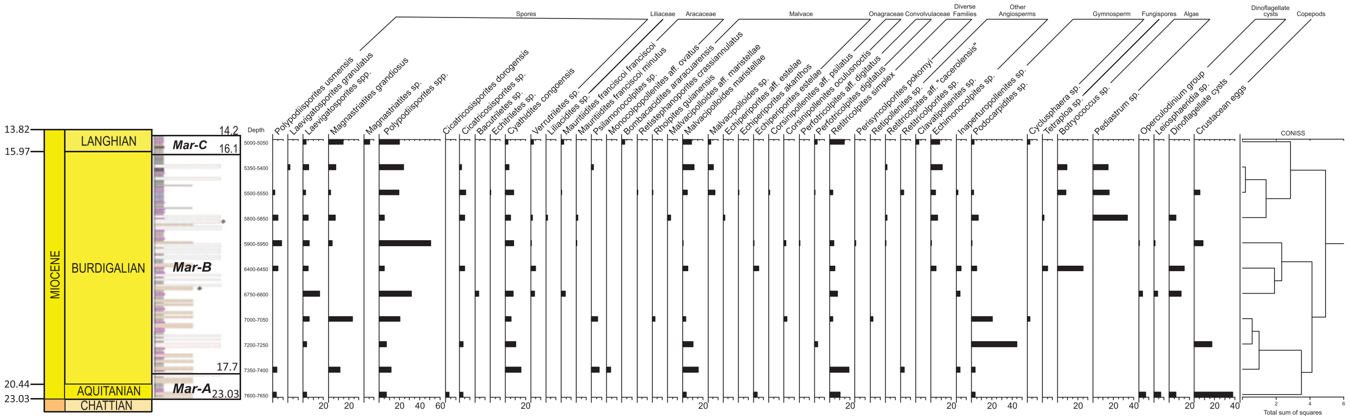

Appendix 4. Tigrillio

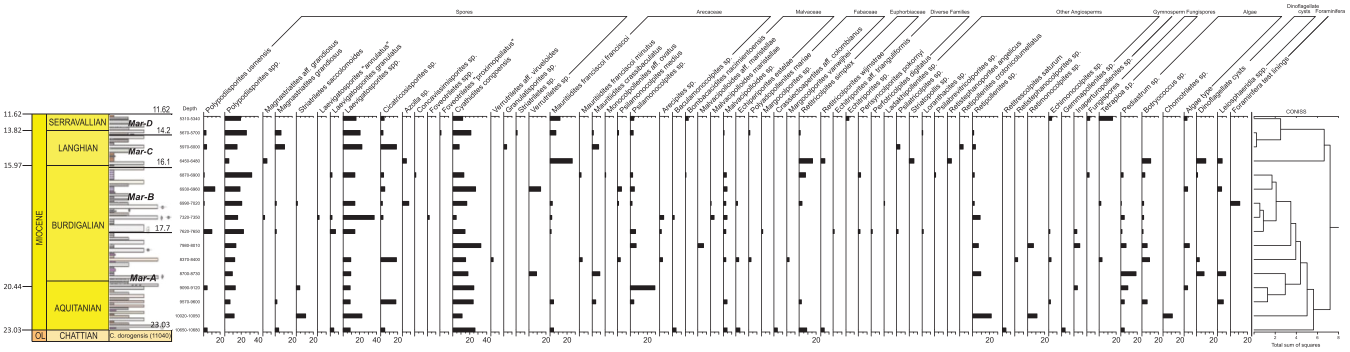

Appendix 5. Nahuapa

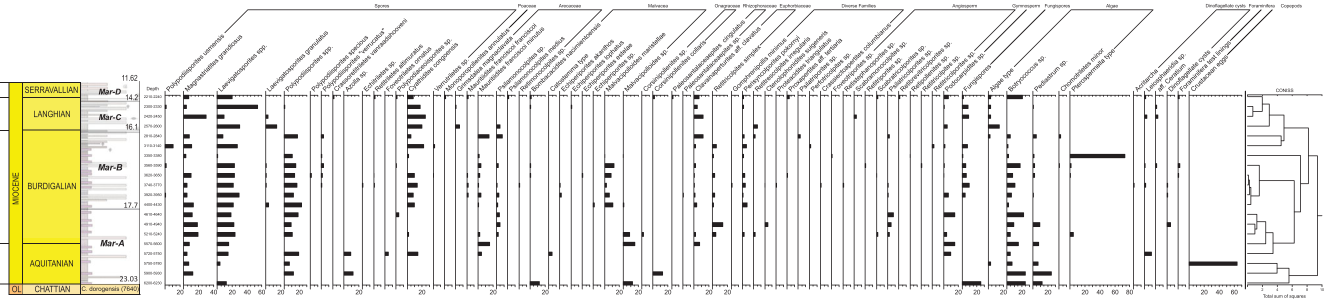

Appendix 6. Frontera